Force-dependent recruitment of Piezo1 drives adhesion maturation and calcium entry in normal but not tumor cells

Mingxi Yao*[1,2,3], Ajay Tijore[3,4], Delfine Cheng[5], Jinyuan Vero Li[5], Anushya Hariharan[3], Boris Martinac[5], Guy Tran Van Nhieu[6], Charles D Cox*[5] & Michael Sheetz*[3,7,8]

1. Department of Biomedical Engineering, Southern University of Science and Technology
2. Guangdong Provincial Key Laboratory of Advanced Biomaterials
3. Mechanobiology Institute, National University of Singapore Mechanobiology Institute, National University of Singapore
4. Centre for Biosystems Science and Engineering, Indian Institute of Science, Bangalore, 560012, India
5. Victor Chang Cardiac Research Institute, Sydney, Australia
6. Ecole Normale Supérieure PARIS-SACLAY
7. Dept of Biological Sciences, National University of Singapore
8. Molecular MechanoMedicine Program, Dept. of Biochemistry and Molecular Biology, University of Texas Medical Branch

*Correspondence: yaomx@sustech.edu.cn, C.Cox@victorchang.edu.au or misheetz@utmb.edu

Abstract:

Mechanosensing is an integral part of many physiological processes including stem cell differentiation, fibrosis, and cancer progression. Two major mechanosensing systems – focal adhesions and mechanosensitive ion channels, can convert mechanical features of the microenvironment into biochemical signals. We report here surprisingly that the mechanosensitive Ca^{2+}-channel Piezo1, previously perceived to be diffusive on plasma membranes, binds to matrix adhesions in a force-dependent manner, promoting adhesion maturation and cell spreading in normal but not in tumor cells. In the absence of Piezo1, matrix adhesions are smaller in normal cells mimicking transformed cells where adhesions do not change with or without Piezo1. A novel adhesion-targeted calcium sensor shows robust Piezo1-dependent, calcium influx at adhesions in normal cells; but not in transformed cells. A linker domain in Piezo1 is needed for binding to adhesions and overexpression of the domain blocks Piezo1 binding to adhesions decreasing adhesion size and cell spread area. Thus, we suggest that Piezo1 is a novel component of focal adhesions in non-transformed cells that catalyzes adhesion

maturation and growth through force-dependent calcium signaling, but this function is absent in most cancer cells.

Introduction

Cellular mechanosensing, the cell's ability to detect and respond to its physical microenvironment, is involved in important processes in development, tissue homeostasis and disease[1,2]. For example, sensing of shear flow in blood circulation is essential for the proper development of vasculature and the depletion of rigidity sensors enables cancer neoplastic transformation, i.e. substrate-rigidity-independent growth[3,4]. Mechanosensitive ion channels and cell adhesions, are major mechanosensors that are responsible for converting mechanical cues into biochemical signals in these processes[5].

A mechanosensing function of focal adhesions is manifest by rigidity-dependent adhesion assembly and turnover, which involves hundreds of different focal adhesion proteins that alter cell behavior during spreading and migration[1]. In addition, focal adhesion mechanosensing regulates pathways such as AKT, MAPK and Hippo-signaling that influence cell fate decisions[1,6,7]. Because adhesions affect cell behavior and fate, the molecular components and dynamics of focal adhesions have been extensively studied. There exists a robust process of adhesion protein recruitment and processing in the finely tuned steps of focal adhesion formation, growth and turnover that correlates with cell state decision making based on cell-microenvironment interactions[8]. There is evidence for force-sensing proteins such as talin and vinculin regulating the functions of focal adhesions as well[2,8–13]. In contrast, although the ion conduction properties of many mechanosensitive ion channels are well-characterized by structural and patch-clamp studies, the mechanisms for converting matrix forces to channel gating are not well understood[14]. This is partly due to the complex nature of ion channel signaling and mechanically-induced calcium influx. For example, mechanosensitive channels are linked to both cell proliferation and apoptosis depending on the context, suggesting that both the distribution and dynamics of the mechanosensitive ion channels are important for understanding the critical mechanosensing processes of the cell.[15,16]

54 There is ample evidence of a crosstalk between mechanosensitive ion channels and focal adhesions. Local
55 calcium entry is critical for focal adhesion assembly and disassembly based upon the calpain dependence of
56 both processes [17–21]. In adhesion assembly during cell spreading, rigidity sensing involves force-dependent
57 calpain cleavage of talin, which is needed for normal adhesions to form and for normal cells to grow[20]. In
58 contrast, transformed cells do not sense matrix rigidity and adhesions are significantly smaller even though
59 tumor cells develop higher traction forces[22]. This raises questions of whether or not transformed cells use
60 calcium in adhesion assembly like normal cells. In addition, several studies found that adhesion disassembly
61 depends upon force-dependent calpain cleavage[18,19]. Thus, there are critical roles for calcium entry in normal
62 adhesion dynamics that are altered in transformed (tumor) cells and the analysis of the channels involved can
63 reveal important aspects of the life cycle of focal adhesions.

64 Several calcium-permeable channels have been implicated in focal adhesions dynamics [23–27] . One of those,
65 Piezo1, is particularly interesting, as early reports of Piezo1 document an interaction with integrins[28]. Piezo1
66 has subsequently been identified as a bona-fide mechanosensitive ion channel in mammalian cells[29]. Since
67 then, Piezo1 has been shown to have many roles in important biological processes and there is increasing
68 interest in how it functions[15,29–31]. Piezo1 is widely expressed in somatic cell types and is linked to
69 mechanosensing in stem cell lineage determination, blood pressure regulation, activation of innate immunity
70 and vascular development[4,30,32,33]. Piezo1's activity has been shown to be related to the integrin-linked actin
71 cytoskeleton [26,34,35]. When Neuro2A cells are mechanically agitated with micron-sized, collagen IV or Matrigel
72 coated beads, the tension threshold required to trigger Piezo-dependent Ca^{2+} entry is significantly reduced[36].
73 In addition, integrin signaling pathways are critical for proper function of Piezo1 in the context of endothelial
74 cell responses to flow[37]. Consequently, we want to investigate the possible crosstalk between Piezo1 and focal
75 adhesions.

76 In this study, we show that in normal cell lines Piezo1 is needed for mature adhesion assembly and it
77 localizes to adhesions as the adhesions mature in a calpain-dependent process, which has been previously
78 observed in the context of talin cleavage[20]. In normal cell lines from many tissues, Piezo1 is enriched at focal

79 adhesions in a force-dependent manner and dissociates after the integrin adhesions disassemble. Its
80 localization correlates with local calcium entry and adhesion disassembly in a calpain-dependent process.
81 Alternatively, in transformed cells, Piezo1 is diffusely distributed and does not affect either adhesion assembly
82 or disassembly and there is low adhesion calcium entry. These studies indicate that Piezo1 normally interacts
83 with adhesions transiently during assembly and then its force-dependent recruitment to mature adhesions
84 catalyzes calpain-dependent adhesion disassembly. These dynamic adhesion interactions are lost in
85 transformed cells and are likely a key neoplastic modification.

86 # *Results*

87 ## *Piezo1 stably localizes to mature adhesions in HFF cells*

88 To investigate the role of Piezo1 in adhesion formation, we followed the distribution and dynamics of
89 Piezo1 localization during cell spreading in Human Foreskin Fibroblast (HFF) cells using total reflection
90 fluorescence microscopy (TIRFM). Transiently expressed Piezo1 tagged with GFP[38] or mRuby3 and paxillin-
91 BFP were followed during the cell spreading in HFF cells (Figure 1A top panel, supplementary movie 1). In
92 the initial phase of spreading, Piezo1 did not colocalize with cell adhesions marked by paxillin and it
93 appeared concentrated around the nucleus. After 30-60 minutes when the cells developed mature
94 adhesions, Piezo1 dispersed to the entire spread area of the cell and was significantly enriched in maturing
95 adhesions.

96 Piezo1 localization to adhesions increased over time until the cell began to polarize. Upon cell
97 polarization, Piezo1 prominently localized to the retracting edges (Figure 1B, upper panel). After spreading
98 overnight, HFF cells reached a dynamic steady state and Piezo1 was enriched at mature focal adhesions
99 (Figure 1B, middle panel). In most cells, Piezo1 was recruited to a sub population of the focal adhesions,
100 mostly around the cell periphery at the ends of stress fibers. Quantification of the extent of Piezo1
101 recuitment to focal adhesions by the ratio of Piezo1 intensity in the adhesion to that in the plasma
102 membrane background showed that the recruitment of Piezo1 to adhesions increased over time as cells

103 spread further and started to polarize (Figure 1 C-D). Piezo1 was often recruited to a portion of individual
104 adhesions as well (Figure 1B lower panel, marked by arrow), implying that the regulation of Piezo1
105 recruitment happened locally. The localization of endogenous Piezo1 to adhesions in HFF cells was also
106 observed by Piezo1 immunostaining of fixed HFF cells (Figure S1) using two knockdown/knockout validated
107 antibodies[15]. Thus, Piezo1 complexed with mature and retracting adhesions in polarized cells on fibronectin.

108 Since Piezo1 was previously reported to be diffusive in plasma membranes[26], we confirmed that the
109 Piezo1 recruitment involved immobilization by checking the lifetime of Piezo1 in the focal adhesions of HFF
110 cells through Fluorescence Recovery After Photobleaching (FRAP). Surprisingly, as shown in Figure 1E, Piezo1
111 was stable at the adhesions after recruitment, with lifetimes of around 120 s that were considerably longer
112 compared to typical focal adhesion proteins such as paxillin ~25 s and even slightly longer than integrins
113 such as integrin β3 ~90 s (Figure 1F). In addition, the mobile fraction of Piezo1 was considerably less than the
114 mobile fraction of paxillin and even integrin β3 (Figure 1F). These data indicated that Piezo1 formed stable
115 interactions with certain focal adhesion components in HFF cells.

116 *Piezo1 recruitment to adhesions requires myosin II contractility*

117 Since focal adhesion maturation was linked to sustained traction forces and correlated with Piezo1
118 recruitment during spreading, we hypothesized that Piezo1-adhesion interactions were force dependent.
119 Treatment of Piezo1-GFP expressing HFF cells with 30 uM of Y23762 to inhibit actomyosin contraction,
120 caused rapid loss of Piezo1 from adhesion sites and was followed by the disassembly of focal adhesions as
121 measured by paxillin (Figure 2A, top panel, supplementary movie2). Similar results were observed with 50
122 μM blebbistatin treatment (Figure S2A). When Y-23762 was washed out, Piezo1 returned rapidly to the
123 reforming adhesions (Figure 2A, top panel). Since Piezo1 recruitment during recovery was much more rapid
124 than the initial recruitment to adhesions during cell spreading (minutes versus hours), we postulated that
125 components remaining at adhesions in the absence of force catalyzed the rapid recovery of adhesion
126 proteins with the development of contractile forces to enable Piezo1 binding. Further, when the

127 contractility of the cell was enhanced by co-expressing the constitutively active version of RhoA along with
128 Piezo1 in HFF cells, the enrichment of Piezo1 at adhesions was strongly promoted (Figure 2A, bottom panel).

129 To check whether the reduction of traction forces alone could disrupt Piezo1's adhesion recruitment
130 without disruption of adhesion proteins such as talin and integrins, we tested the relationship between
131 Piezo1 localization and myosin II contractility in intact adhesions. Previous reports showed that inhibition of
132 the tyrosine phosphatase, PTP-PEST, as well as the expression of virulence bacterial protein IpaA, inhibited
133 adhesion disassembly upon addition of Y-23762 [39,40]. In cells expressing GFP-labelled IpaA peptide, addition
134 of 30 µM Y-23762 caused cells to lose contractility while retaining adhesion structures (Figure 2B,
135 Supplemental movie 3). In this case, Piezo1-mRuby3 diffused out from adhesions within 10 min after Y-
136 23762 addition while the integrin β3-BFP remained intact. A similar effect was observed when 2.5 µM of
137 PTP-PEST inhibitor was added in combination with 30 µM Y-23762 (Figure S2B). Thus, the localization of
138 Piezo1 to focal adhesions depended on continued contraction forces possibly through the stretching of
139 adhesion proteins, and was independent of paxillin or integrin β3 localization to adhesions.

140 To further establish the role of myosin II-based contractility in Piezo1 recruitment, we checked the
141 distribution of Piezo1 in cells that had low traction forces such as COS-7 cells lacking myosin IIA expression[41].
142 In COS-7 cells transiently expressing Piezo1-GFP and paxillin-mapple, Piezo1 was diffusive in the membrane
143 with no apparent localization to adhesions (Figure 2C, top panel) and the cell adopted a highly-spread disc
144 morphology. When contractility was restored in COS-7 cells by overexpressing myosin IIA, cells became
145 polarized with myosin IIA forming stress-fiber-like cables (Figure 2C, bottom panel) and Piezo1 was recruited
146 to the adhesions at the ends of the myosin cables. This further reinforced the hypothesis that Piezo1
147 recruitment to adhesions required continued force on the adhesion complex.

148 *Piezo1 recruitment triggers (calpain dependent) integrin β3 adhesion turnover*

149 Since Piezo1 was recruited to only a fraction of focal adhesions, we proceeded to check whether
150 different integrin subtypes played a role in the regulation of Piezo1 localization. As shown in Figure 3A, we
151 transiently expressed Piezo1-1591-mRuby3 with integrin β3-mEmerald and analyzed the colocalization of

152 Piezo1 with β3 adhesions during cycles of adhesion assembly and disassembly. Interestingly, the recruitment
153 of Piezo1 to β3-enriched adhesions correlated with the disassembly and turnover of the β3 adhesions. Figure
154 3A shows the timelapse views of two such turnover events on fibronectin surfaces, one during spreading
155 where the cell was protruding and the other in migrating cells where the adhesion was retracting. In both
156 cases, integrin β3-based adhesions formed without apparent Piezo1 co-localization. Over time, Piezo1 was
157 recruited to the adhesions from the periphery of the adhesions and gradually occupied the whole adhesion.
158 Piezo 1 recruitment appeared to initiate a decrease in integrin β3 fluorescence intensity within minutes
159 (Figure 3A and supplementary movie 4-5). After integrin β3 reached background levels, the Piezo1
160 fluorescence often persisted in adhesions for a few minutes before dissociation (Figure 3A, Left panel,
161 arrows; Figure S3A gives a detailed profile), suggesting that some adhesion components remained that
162 supported Piezo1 localization after integrin β3 dissociated from the adhesion.

163 In contrast, the anticorrelated behavior was not observed between Piezo1 and β1 integrins in adhesions.
164 Piezo1 recruitment at integrin β3 and β1 enriched adhesions was more stable, and they often co-localized
165 for tens of minutes (Figure S3B). In an interesting example (Figure S3B), Piezo1 recruitment correlated with
166 the rapid dissociation of β3 integrins and enrichment of β1 integrins. Piezo1 recruitment persisted in
167 adhesions even after dissociation of β3 integrins (Fig. S3B, arrows). These observations indicated that Piezo1
168 recruitment was associated with adhesion turnover that was regulated locally in an integrin β3 dependent
169 manner.

170 Considering Piezo1's function as a mechanosensitive Ca^{2+} channel, adhesion turnover was likely caused by
171 the calpain-dependent cleavage pathway. Indeed, when we blocked calpain activity using the inhibitor ALLN,
172 adhesion turnover from the back of the sliding adhesions was inhibited, causing significant elongation of the
173 adhesions (Figure S3C, left panel, Supplementary Movie 6). However, the speed of adhesion extension was
174 not altered (Supplementary Movie 6). Piezo1 remained in adhesions following ALLN addition in HFF (Figure
175 S3C). Thus, normal dynamics of β3 adhesions depended upon calpain activity that was likely regulated by
176 local Ca^{2+} entry induced by Piezo1's channel activity.

177 Based upon these findings we hypothesized that Piezo1 recruitment was upstream of calpain in
178 regulating adhesion turnover. In earlier studies of cells on fibronectin, integrin β3 adhesions formed initially,
179 and then the adhesions switched to integrin β1. The greater stability of β1-containing adhesions with Piezo1
180 recruitment could potentially provide a mechanistic explanation for such switching events[42].

181 *Piezo1 localization to adhesions is lost in transformed cells*

182 To check whether Piezo1 localization to adhesions was cell-type specific, we expressed Piezo1 in a
183 variety of normal and transformed cell lines (Figure 4A, Figure S4A). In all of the normal cell lines of
184 fibroblastic (HFF, MCF-10A), epithelial (HUMEC) or endothelial origins (HUVEC), Piezo1 localized to a
185 significant subset of the focal adhesions on fibronectin visualized by paxillin (Figure 4A, Figure S4). In the
186 case of 12 different tumor cell lines from mesenchymal or epithelial tissues (fibrosarcoma, melanoma,
187 breast and lung cancers, Figure 4D), there was no significant colocalization of Piezo1 with paxillin adhesions.
188 In the HT1080 (fibrosarcoma) and MDA-MB-231 (breast cancer) cells, FRAP measurements of Piezo1
189 diffusion showed that Piezo1 had a significantly higher mobile fraction than in HFF cells (Figure 4B). The
190 difference in Piezo1 immobilization was not due to different levels of Piezo1 expression, since Western blots
191 showed significant levels of Piezo1 in most of these cell lines (Figure 1D, Figure S4B). Thus, the colocalization
192 of Piezo1 with adhesions was found only in normal cells. In all of the tumor cells tested, Piezo1 was not
193 colocalizing with adhesions and was rapidly diffusing.

194 Our previous studies showed that TPM 2.1 levels were low in many transformed cells[22]. Knocking down
195 TPM 2.1 in HFF cells caused the cells to become transformed with smaller adhesions and the cells were not
196 able to differentiate between soft and rigid surfaces. In contrast, restoring TPM 2.1 expression in MDA-MB-
197 231 cells caused normal behavior with bigger adhesions and the cells died on soft agar[22]. Based on this, we
198 checked if toggling between the non-transformed and transformed states in HFF and MDA-MB-231 cells
199 altered the localization of Piezo1 in these cell lines. When we knocked down TPM 2.1 in HFF cells, the
200 recruitment of Piezo1 to adhesions was significantly weakened compared with control cells or control siRNA-
201 treated cells (Figure S5 A). In contrast, when we transiently expressed TPM 2.1-YFP in MDA-MB-231 cells, a

202 fraction of cells formed stress fibers and Piezo1 was recruited to adhesions at the end of stress fibers (Figure
203 S5 B). These data indicated that there was a correlation between normal cell behavior and Piezo1 adhesion
204 localization and we recently showed that transformation resulted from the loss of rigidity sensing, which was
205 observed in the majority tumor cells[22]. Thus, the change in cell state from normal to transformed state
206 diminished Piezo1 binding to adhesions.

207 *Piezo1 is needed for adhesion maturation and polarity in normal but not in*
208 *transformed cells*

209 As the pattern of Piezo1 adhesion recruitment differs in normal and transformed cell lines, we checked if
210 Piezo1 regulated focal adhesion morphology differently in normal and transformed cell lines. To minimize
211 the possibility of cell-type variance, we used normal primary cells and transformed cancer cells of matching
212 origin (Human foreskin fibroblast with HT1080 human fibrosarcoma). As shown in Figure 5A, Piezo1 knock-
213 down HFF cells spread to smaller areas, had a lower aspect ratio and had smaller adhesions, while in the
214 transformed HT1080 cells, knocking down of Piezo1 caused a significant increase in cell spread area but had
215 no effect on aspect ratio or adhesion size (Figure 1 A-C).

216 This indicated that Piezo1 was important for adhesion maturation and cell polarization in normal cells
217 but had little effect on adhesion formation in transformed cells, while affecting spreading area. Previous
218 studies documented that transformed cell lines including cancer cells generally had smaller and less mature
219 adhesions compared with non-transformed cells[22,43]. This was despite the fact that the majority of adhesion
220 components were present at similar levels in both normal and transformed cells[44,45]. Thus, Piezo1
221 recruitment to adhesions in normal cells appeared to be involved in important steps in the adhesion
222 maturation process whereas in transformed cells, Piezo1 depletion caused no change in adhesion
223 morphology[46].

224 *Piezo1's adhesion recruitment leads to local calcium transients around adhesions in*
225 *normal but not in transformed cells.*

226 Next we checked the possible physiological significance of the Piezo1 adhesion recruitment. Since Piezo1
227 functions as a mechanosensitive ion channel, the recruitment of Piezo1 to adhesions may have altered the
228 calcium entry pattern of the cells. Recent studies by Ellefsen et. al, showed that Piezo1-dependent calcium
229 spikes were localized to the cell periphery near focal adhesions[26]. This implied that calcium spikes occurred
230 near where there were concentrations of Piezo1 at adhesions. Because Piezo1 was not concentrated in
231 adhesions of transformed cells such as MDA-MB-231 and HEK293T, there was a question of whether or not
232 similar calcium spikes would occur near adhesions in transformed cells.

233 To determine if calcium entry near adhesions in fibroblasts also occurred in tumor cells, we loaded HFF
234 and MDA-MB-231 cells with the cell-permeable calcium indicator Cal-520 and imaged transient calcium
235 "puffs" on fibronectin surfaces. Similar to previous observations in HFF cells[26] , many local calcium entry
236 events were detected in areas of high contractility at the cell edge and surrounding adhesions (Figure S6).
237 Interestingly, although the transformed MDA-MB-231 cells generated higher local traction forces[22] and
238 were killed by calcium-dependent apoptosis after stretch[16], they had very few calcium spikes on fibronectin
239 surfaces (Figure S6). This indicated that the calcium influx in cancer cells was abnormal and was consistent
240 with the lack of Piezo1 within adhesions after transformation.

241 Although the measurements with Cal-520 calcium sensor provided interesting insights into the
242 differences in spatial calcium signaling between normal and transformed cells, there remained several
243 specific questions about whether these calcium fluctuations were localized to sites of adhesion. The
244 diffusive nature of all Ca^{2+} dyes reduces the signal-to-noise ratio for calcium influx at sub-cellular locations,
245 providing only limited spatio-temporal information on local Ca^{2+} changes. In addition, under imaging
246 conditions sensitive to subcellular calcium events, Cal-520 had significant photo toxicity that caused rapid
247 increases in intracellular calcium levels limiting the observation window. To better quantify and understand
248 the details of calcium entry at the adhesions, we generated a novel focal adhesion targeted calcium sensor,
249 in which one of the latest most sensitive recombinant calcium sensors, jGCaMP7s, was linked to a paxillin
250 mScarlet-I construct[68]. This improved the signal-to-noise ratio specifically at the adhesions, and the ratio

251 between the calcium sensor and the mscarlet-I fluorescence enabled normalization of the calcium levels
252 based on the local sensor concentration.

253 When the paxillin calcium sensor was transfected in HFF, HT1080 and MDA-MB-231 cells, it localized
254 robustly to apparent adhesions. After overnight spreading, the intensity ratio of jGCaMP7s and mScarlet-I in
255 the focal adhesions of HFF cells showed frequent calcium spikes (Figure 6 A ,supplementary movie 7). The
256 calcium fluctuations were greatly reduced in Piezo1 knock down cells, indicating that Piezo1 was required for
257 the calcium fluctuations around the adhesions(Figure 6 A ,supplementary movie 8). Interestingly, in the
258 transformed HT1080 and MDA-MB-231 cells the calcium spikes at the adhesions were significantly weaker,
259 often there was no detectable calcium signal during a 1-hour observation window(Figure 6 A ,supplementary
260 movie 9-10). In the transformed cells, matrix adhesions still formed and disassembled, suggesting that
261 calcium entry around adhesions was not required for adhesion turnover in the transformed cells. These
262 results indicated that Piezo1 recruitment to adhesions in HFF cells enabled calcium spikes that could in turn
263 induce calpain-dependent adhesion turnover; but in transformed cells, adhesion dynamics and cellular
264 calcium fluctuations were de-coupled.

265 *The central linker domain (1418-1656) of Piezo1 is required for Piezo1 adhesion*
266 *recruitment and alters cell morphology of non-transformed cells*

267 We proceeded to investigate potential molecular mechanisms of Piezo1 adhesion recruitment. So far, no
268 binding partners of Piezo1 at focal adhesions have been reported in the literature. The long lifetime of Piezo1
269 at the adhesions and the dependence of Piezo1 recruitment on actomyosin contractility led us to hypothesize
270 that Piezo1 bound to adhesion-linked components of the actin cytoskeleton stretched by cellular contractility.
271 Upon examining the 3D architecture of Piezo1[47], we identified a long intracellular linker as a potential
272 interaction site between Piezo1 and the actin cytoskeleton.

273 This long intracellular linker region was largely unresolved in the Cryo-EM structures and connected the
274 beam to the clasp and via another unresolved loop to Piezo1 repeat B[47,48]. Previous biophysical studies showed

275 that deletions at the proximal portion of the loop influenced the biophysical properties of the channel via
276 effects on the latch domain[49]. However the distal end was not explored in those studies.

277 To check the potential function of the linker region of Piezo1, we first made a mNeongreen construct of the
278 larger region of human Piezo1 (residue 1418-1656;mNeonlinker) that contained the unstructured loop region,
279 the clasp and a second disordered loop previously shown to be able to house fluorescent tags[38]. We next
280 checked for its localization and interaction with Piezo1. As shown in Figure 7A, the mNeonlinker construct
281 expressed in HFF cells appeared to be diffusely distributed with no apparent concentrations. However, Piezo1
282 recruitment to adhesions was reduced as was adhesion size with overexpression of the mNeonlinker (Figure
283 7A). This is consistent with the hypothesis that at high expression levels the mNeonlinker domain acted as a
284 dominant negative competitor and displaced Piezo1 from adhesions. When we checked the morphology of
285 the cells, HFF cells had significantly lower cell spread area and aspect ratio with the mNeonlinker over-
286 expression, which resembled the morphology change of HFF cells after Piezo1 knock-down. These results were
287 consistent with the hypothesis that the recruitment of Piezo1 to focal adhesions in non-transformed cells
288 activated local calcium fluctuations in surrounding adhesions, and the calcium signal led to adhesion
289 maturation and cell polarization. In the case of transformed cells where Piezo1 did not localize to adhesions,
290 expression of mNeonlinker should have caused minimal effect on cell morphology. Indeed, expression of
291 mNeonlinker in HT1080 cells caused no change in morphology, cell spread area or aspect ratio compared with
292 controls (Figure 7A-C).

293 To further check if this linker region of Piezo1 indeed harboured focal adhesion binding sites, we generated
294 several Piezo1 mutants with the linker regions deleted (short: Piezo1 Δ1443-1556and long: Piezo1 Δ1443-
295 1473). The Δ1443-1473 deletion removed the loop region and the longer Δ1443-1556 mutant removed much
296 of the clasp domain. When we expressed these deletion mutants in FAK -/- MEF cells that had prominment
297 recruitment of WT Piezo1 to adhesions, we observed normal Piezo1 adhesion recruitment of Piezo1 Δ1443-
298 1473 mutant and diffusive Piezo1 localization of the Δ1443-1556 mutant (Figure S7 and supplementary

299 movie11-12). Electrophysiological characterization in Piezo1 KO HEK293T cells showed that the Δ1443-1473
300 mutant had normal stretch induced channel activity while the Δ1443-1556 mutant was not functional.

301 Taking these data together, it appeared that the linker domain(residues 1418-1656) and most likely the clasp
302 region of Piezo1 harbored a binding site for focal adhesion components that recruited Piezo1 to focal
303 adhesions in a force-dependent manner in non-transformed cells at the membrane-cytoplasm interface.

304 *Discussion*

305 In this study, we show that Piezo1 has important functions in focal adhesion dynamics in normal cells
306 but not in transformed cells. Normal fibroblasts, epithelial and endothelial cells form focal adhesions on
307 fibronectin where Piezo1 concentrates in a force-dependent process. The lifetime of Piezo1 in the adhesions
308 is similar to that of integrins and longer than typical adhesion proteins, which implies that it complexes
309 stably with adhesion bound proteins. Sustained contraction forces are needed for piezo1 localization to
310 adhesions; and when contraction is inhibited, it could leave adhesions before the dissociation of adhesion
311 components such as integrin and talin. Piezo1 localization to focal adhesions leads to the dissociation of
312 integrin β3 containing adhesions but not integrin β1 adhesions on fibronectin. This localization is also lost in
313 transformed cells, including virus-transformed somatic cells (e.g. HEK293T) as well as tumor cell lines from
314 different tissues. When somatic cells are transformed such as in the case of TPM 2.1 knock down, the
315 recruitment of Piezo1 to adhesions is dramatically reduced similar to the transformed cancer lines tested.
316 Calcium levels in the vicinity of adhesions are higher and have many more local fluctuations in normal cells
317 compared with transformed cells. Binding to adhesions depends upon an unstructured cytoplasmic domain
318 of Piezo1 (aa 1418-1656). These findings indicate that Piezo1 has a number of complex interactions, which
319 depend upon contractility, the transformed state, as well as specific integrin-matrix interactions. Piezo1
320 appears to have multiple context-dependent functions in normal and transformed cells that need to be
321 analyzed temporally and spatially in a defined mechanical environment.

322 Piezo1 was first identified as an integrin-interacting protein which had a role in adhesion formation[28].
323 Our results reinforce those findings and further indicate that Piezo1 binds in a complex with integrins but
324 not with adhesion proteins such as talin or paxillin, which have much more rapid recovery rates after
325 photobleaching. Further, inhibition of PTPN12 activity or expression of the *Shigella* IpaA effector stabilizes
326 adhesion proteins even after inhibition of myosin but does not prevent Piezo1 dissociation. Piezo1's rapid
327 dissociation upon myosin inhibition is rapidly reversed upon washout of the myosin inhibitor. The rate of
328 return to the adhesions is much more rapid than during initial adhesion formation, indicating that the
329 recruitment of Piezo1 at adhesions depends on a force-sensitive protein or activation of a force-dependent
330 enzyme that is retained at adhesion sites during myosin inhibition. Overexpression of a linker region of
331 human Piezo1 acts as a dominate negative, displacing Piezo1 from adhesions, implying that this linker region
332 of Piezo1 harbours the interacting site for adhesion binding. The lack of adhesion maturation after depletion
333 of Piezo1 strongly supports the hypothesis that Piezo1 has an important role in the force-dependent
334 maturation of adhesions on rigid surfaces, and this does not occur in transformed cells.

335 Since the discovery of Piezo1's role as a mechanosensitive ion channel in eukaryotic cells, the regulation
336 mechanism of Piezo1's function in the various physiological activities of cells has been under heavy
337 investigation[50,51]. The classical model of Piezo1's physiological function assumes that it is diffusive in the
338 plasma membrane and is activated locally through membrane bilayer tension or curvature changes that
339 occur through cytoskeletal-dependent mechanical events[26,34,38,47,52]. Several recent studies have clearly
340 shown that the cystoskeletal environment influences Piezo1 function[38], including the observation that
341 Piezo1 localizes to the adhesions of some glioblastoma cell lines, which facilitates their growth and
342 invasion[27]. The unusual nature of these glioblastoma lines indicates that they may be more like normal cells
343 than transformed cells (Yao et al unpublished results). In our study, we systematically examine Piezo1's
344 spatial distribution across many cell types from different tissues of origin and discover that Piezo1 adhesion
345 localization is much more prominent in non-transformed normal cells compared with transformed cells such
346 as most tumor cell lines. Binding to the adhesions in normal cells catalyzes adhesion maturation and
347 disassembly that correlates with cell growth.

348 Interestingly, in contrast to the reduced calcium transients that we observed in resting transformed
349 cells, we recently reported that mechanical perturbations, such as stretching or ultrasound treatment, cause
350 Piezo1-dependent increases in cytoplasmic Ca^{2+} levels and subsequent apoptosis of transformed but not
351 normal cells[53]. These observations are difficult to explain in terms of fluctuations in either mechanical forces
352 on adhesions or membrane tension, especially since fewer Ca^{2+} fluctuation events are observed in
353 transformed cells whereas Ca^{2+} flickering events near adhesion sites are common in normal cells. With
354 regard to membrane tension, typical measurements of membrane tension in cells report values that are 2-3
355 orders of magnitude smaller than those needed to activate Piezo1 in vitro[54,55]. Certainly, the pattern of Ca^{2+}
356 activation in the HFF cells in the vicinity of adhesions is consistent with previous results[46,56,57], but it is not
357 consistent with the simplistic model of very high membrane tension for the whole cell. Rather, there appear
358 to be local activation events that involve elements from the adhesions that may alter local membrane
359 tension/curvature or the association of membrane/cytoskeletal proteins that can modulate the mechanical
360 gating of Piezo1 activity[52,58,59]. Although Piezo1 appears in many different mechanical functions, the
361 activation mechanism of Piezo1 is complex and both contributions from membrane tension and interaction
362 with cytoskeletal proteins may modulate its activity[35,58].

363 We recently showed that transformed cancer cells are depleted of the rigidity sensing, local contraction
364 units[22,43]. There is a conserved set of cytoskeletal proteins that are able to assemble into local rigidity sensing
365 contractile structures in normal cells. After the depletion of any one of several cytoskeletal proteins critical
366 for rigidity sensing and contractile pair assembly, the cell will be transformed and will no longer sense
367 substrate rigidity. Transformation also involves changes in adhesion morphology and composition[22]. The
368 differences in the adhesion components in normal and transformed cells that contribute to the adhesion
369 phenotype are still an open question but the mRNA levels of over 700 proteins are altered upon
370 transformation by tropomyosin 2.1 depletion[22]. An important function of the rigidity sensors is in the
371 maturation of focal adhesions that contain Piezo1 and without Piezo1 the mature adhesions do not form.
372 This further fits with the absence of any differences between transformed cell adhesions with and without
373 Piezo1. Thus, we suggest that normally both the maturation and the disassembly of focal adhesions is

374 catalyzed by Piezo1. In addition, whether the differences in Piezo1 recruitment in the transformed and
375 somatic cell lines are caused by changes in the molecular interactions or tension states of these cells remains
376 an open question and awaits further investigation.

377 Our model of the function of Piezo 1 in Figure 8 emphasizes the catalytic role of Ca^{2+} entry in the life
378 cycle of the adhesions in normal cells. Initially, the nascent adhesions seed actin filament formation, myosin
379 bipolar filaments pull on the actin in the rigidity-sensing contractions, and there is a calcium-dependent
380 cleavage of talin1 that is needed for growth[8,20]. If the matrix is rigid, then adhesions mature through
381 enzymatic modifications that trigger the maturation process. Components in the adhesions are stretched by
382 traction forces and then can bind Piezo1 which permits Ca^{2+} entry in a positive feedback cycle for the further
383 maturation of the adhesion. However, when the concentration of Piezo1 reaches a threshold, there is
384 excessive Ca^{2+} entry and recruitment of calpain that now hydrolyzes components of the adhesion, causing
385 the disassembly of the adhesion. The maturation process requires the rigidity sensing complex and will not
386 occur in transformed (cancer) cells. This model indicates that covalent modification of adhesion
387 components during maturation as well as traction forces on those components are necessary for Piezo1
388 binding. Further understanding of Piezo1 functions requires dynamic studies of Piezo1 at the appropriate
389 time and location during cell spreading or migration.

390 There is growing evidence that covalent modifications in maturing adhesions alter adhesion proteins as
391 well as possibly membrane proteins in normal cells[20,60]. The release of Ca^{2+} near adhesions contributes to
392 protein processing by the adhesion signaling hub, which is needed for adhesion maturation and cell growth
393 on a rigid fibronectin matrix possibly through a localized calpain-dependent pathway. The paxillin-associated
394 calcium indicator shows that the Piezo1-dependent influxes of calcium are much more numerous than
395 observed with the cytoplasmic calcium indicator. Thus, the localization of Piezo1 to the adhesions under
396 force will provide a very localized activation of calpain and other calcium-dependent enzymes to modify
397 adhesions and membrane proteins in specific locations.

398 In transformed cells, growth appears independent of local Ca^{2+} entry at rigid matrix sites and Piezo1 is
399 decoupled from traction forces and adhesion signaling. It is commonly believed that transformed cells are
400 related to wound healing where cell growth for repair is needed and localized signaling from matrices is not
401 needed[61] . Further, in many cancers, the elevated growth rates correlate with high levels of calpain that
402 could amplify small Ca^{2+} leaks to support the growth activity. This could help to explain how stretch could
403 cause general changes in the plasma membrane activating Ca^{2+} entry through Piezo1 by local membrane
404 tension or curvature changes that would cascade into an apoptotic process[16]. Most importantly, the general
405 activation of growth in cancer cells appears to occur without localized signaling at adhesions by Piezo1.

406 In the larger picture of adhesion maturation, there are many adhesion proteins that bind to adhesions in
407 a force-dependent manner[62,63]. It is surprising, however, that the inhibition of the release of many adhesion
408 proteins by the inhibition of PTPN12 or expression of virulence bacterial protein IpaA did not block the
409 release of Piezo1 upon myosin inhibition. Further, Piezo1 is strongly bound to the adhesions and has a
410 lifetime similar to integrin beta3 in adhesions that depends on contractility. The stronger retention of Piezo1
411 at adhesions upon the transition from integrin beta3 to beta1 may aid in the stabilization of such adhesions
412 for development of higher forces on matrix contacts through continued local influx of calcium[64]. The
413 integrin subtype dependence of Piezo1 dynamics could be of great importance for the physiological function
414 of Piezo1, e.g. in vascular development[4]. Piezo1 localization likely plays a critical role in processes such as
415 vascular development and tumor angiogenesis where both Piezo1 and β3 integrins are indispensable. Piezo1
416 knock-out mice die as embryos due to vascular defects, and inactivation of beta3 inhibits the angiogenesis
417 process. Mechanical forces such as shear forces are very important in these processes[4]. The force dependent
418 co-localization and turnover of Piezo1 at β3 integrin adhesions could be synergistic with downstream events
419 and provides a mechanism of tension-dependent vascular growth that is critical in development. Thus, we
420 suggest that the contractility dependent recruitment of Piezo1 to focal adhesions is a novel crosstalk
421 mechanism between the two major mechanotrasduction hubs of the cell that play critical roles in adhesion
422 function and are lost in most tumor cells (Figure 8) .

423 # *Material and methods*

424 ## *Cell culture and constructs:*

425 The mEmerald-integrin β3, mEmerald-integrin β1, paxillin-mapple, paxillin-BFP and talin-GFP were gifts
426 from Michael Davidson (Addgene plasmid # 56330, #54129, #54935). The piezo1-GFP-1591 and piezo1-
427 mruby3-1591 plasmids were generated as previously described[38]. The RhoAV14 construct was from
428 Schwartz lab[65]. TPM2.1-YFP construct was from Gunning Lab[66]. The A431 ipa peptide plasmid was generated
429 as previously described[67]. The paxillin calcium sensor was generated by PCR cloning of jGCaMP7s segment
430 from pGP-CMV-jGCaMP7s plasmid from addgene[68] and inserted into the N-terminal of a paxillin-mScarleti
431 construct derived from paxillin-mapple.

432 siRNA for tropomyosin 2.1 was synthesized as previously described by Dharmacon[43]. siRNA for human
433 Piezo1 was ordered from Dharmacon (ON-TARGETplus human Piezo1 siRNA, SMARTpool, L-020870-03-0010)
434 and Merck Sigma-Aldrich (SASI_HS01_00208585) or Life Technologies(cat no #21816). RT-PCR analysis
435 showed that both siRNA caused >90% knock down at the mRNA level two days after transfection. The siRNA
436 were transfected using RNAiMAX reagent from ThermoFisher following manufacture's protocols.

437 Human Foreskin fibroblast (HFF), HUMEC, HUVEC, HT1080, A2058, A375P, and MCF-10A cells were
438 obtained from ATCC. MDA-MB-231, SKOV3, cells were from Ruby Huang's lab. HEK293T cells with piezo1 KO
439 were from Ardem Patapoutian's lab. HFF, MDA-MB-231, HEK293T Piezo1 KO and cells were cultured in 1X
440 DMEM supplemented with 5 mM sodium pyruvate and 10% of Hi-FBS. MCF-10A cells were cultured using
441 fomulated media as reported previously[22] and HUVEC cells were cultured in endothelial growth media from
442 Sigma.

443 ## Ca^{2+} *influx measurements*

444 For calcium level measurements using force sensors, cells were transfected with the GCAMP7S-paxillin-
445 mScarleti construct and seeded on fibronectin coated glass bottom coverslips overnight. Transfected cells
446 were imaged using TirfM microscrope using 488 and 561 laser lines. Specific band pass excitation/emission

447 filter cubes (GFP-HQ and mCherry-HQ from Nikon) were used to avoid fluorescence crosstalk between
448 channels. For comparison between different samples, all imaging parameters (laser power, tirf angle,
449 camera exposures) were kept constant. Only cells with comparable calcium sensor expression levels (judging
450 from fluorescence intensity from mScarlet channel) were picked for analysis to minimize potential bias due
451 to sensor concentration differences.

452 The local Ca^{2+} influx of the cells was measured following Ellefsen et. al[26]. Briefly, the HFF cells were
453 loaded with 4 uM Ca^{2+} indicator Cal-520-AM for 2 hours. Then the cells were detached using enzyme free
454 dissociation media and resuspended in complete growth media. The cells were allowed to recover in
455 suspension for 20 min before seeding on glass bottom coverslips coated with fibronectin. After 2 hours the
456 buffer was switched to Ringer's balanced salt and proceeded for imaging on Nikon Tirf system with pulsed
457 laser lines to minimize photodamage of the sample[69]. The calcium images of individuals cells were acquired
458 at 100Hz for 5000 frames. The deltaF/F images of the cells were generated using a custom matlab script to
459 reveal individual Ca^{2+} influx events. Such events were tracked using the Trackmate ImageJ plugin[70].

460 *Cell spreading assay*

461 In the cell spreading assay, cells were transfected with respective plasmids 36-48 hours before
462 experiments using Neon transfection system (Thermo Fisher) or JetOptimus chemical transfection reagent
463 (PolyPlus) following manufacturer's recommendations. On the day of experiment, the cells were detached
464 using an enzyme-free cell detaching buffer (Cell Dissociation Buffer, enzyme-free, PBS, Gibco), spun-down
465 and resuspended in complete media (1X DMEM, 10% FBS). The suspended cells were allowed to recover by
466 incubating in the cell culture hood for 20 min and then seeded onto glass bottom Petri dishes coated with
467 ECM molecules of interest (10 ug/ml collagen I, 10 ug/ml fibronectin, 10 ug/ml VTN-N, and 10 ug/ml laminin
468 for 1 hour). Imaging was done on a Nikon Tirf system with 405,488,561 and 640 laser lines. The cell
469 spreading area and adhesion size were analyzed automatically using CellProfiler[71].

470 *Immunostaining and antibodies*

471 Cells of interest seeded on glass bottom Petri dishes were fixed with 4% paraformaldehyde (PFA) for 30
472 min at 37 degrees and washed with 1X PBS three times. The fixed cells were permeabilized/blocked by
473 incubation with TBST (1X TBS, 0.1% Tween-20) containing 5% Bovine Serum Abumin (BSA) overnight at 4
474 degrees. Primary antibodies were diluted in TBST, 5% BSA solution according to manufactures'
475 recommendations and added to the cells overnight at 4 degrees. The stained cells were washed with 1X PBS
476 and stained with secondary antibody for 1 hour at room temperature.

477 Polyclonal Rabbit and monoclonal mouse anti-Piezo1 was from Novus Biologicals (NBP1-78446, NBP2-
478 75617), both have been validated by Piezo1 knock down/knock off experiments[15,72]. For all Piezo1
479 localization quantifications, the monoclonal NBP2-75617 antibody was used. Mouse anti-Paxillin antibody
480 was from Merck Millipore (MAB 3060), Rabbit anti-paxillin antibody was from abcam(ab32115). Mouse anti-
481 activated integrin β1 antibody was from BD Biosciences (9EG7). Rat anti integrin αvβ3 was from
482 Millipore(LM609).

483 *FRAP analysis*

484 FRAP analyses were carried out on an ILAS2 TIRF image system similar to reported previously. Briefly,
485 HFF, HT1080, or MDA-MB-231 cells transiently co-transfected with Piezo1-GFP and Paxillin-mapple, or
486 Piezo1-mruby3 and mEmerald-integrin β3 were seeded on Fibronectin coated glass bottom dishes overnight.
487 2-5 square-shaped regions of interests (~3 um length) covering focal adhesions were selected for each cell
488 and bleached. The recovery of fluorescence in both fluorescent channels was observed for from 360 to 600
489 seconds after photobleaching. The recovery curves were normalized by dividing by average intensity of each
490 ROI before bleaching and the average and standard deviation of the recovery were calculated.

491 *References*

492 1. Geiger, B., Spatz, J. P. & Bershadsky, A. D. Environmental sensing through focal adhesions. *Nat. Rev.*
493 *Mol. Cell Biol.* **10**, 21–33 (2009).

494 2. Vogel, V. & Sheetz, M. Local force and geometry sensing regulate cell functions. *Nat. Rev. Mol. Cell*
495 *Biol.* **7**, 265–75 (2006).

496 3. Jain, R. K., Martin, J. D. & Stylianopoulos, T. The Role of Mechanical Forces in Tumor Growth and
497 Therapy. *Annu. Rev. Biomed. Eng.* **16**, 321–346 (2014).

498 4. Li, J. *et al.* Piezo1 integration of vascular architecture with physiological force. *Nature* **515**, 279–282
499 (2014).

500 5. Bershadsky, A. D., Balaban, N. Q. & Geiger, B. Adhesion-dependent cell mechanosensitivity. *Annu.*
501 *Rev. Cell Dev. Biol.* **19**, 677–95 (2003).

502 6. Panciera, T., Azzolin, L., Cordenonsi, M. & Piccolo, S. Mechanobiology of YAP and TAZ in physiology
503 and disease. *Nat. Rev. Mol. Cell Biol.* (2017) doi:10.1038/nrm.2017.87.

504 7. Trappmann, B. *et al.* Extracellular-matrix tethering regulates stem-cell fate. *Nat. Mater.* **11**, 642–649
505 (2012).

506 8. Wolfenson, H., Yang, B. & Sheetz, M. P. Steps in Mechanotransduction Pathways that Control Cell
507 Morphology. *Annu. Rev. Physiol.* **81**, 585–605 (2019).

508 9. Horton, E. R. *et al.* Definition of a consensus integrin adhesome and its dynamics during adhesion
509 complex assembly and disassembly. *Nat. Cell Biol.* **17**, 1577–1587 (2015).

510 10. del Rio, A. *et al.* Stretching single talin rod molecules activates vinculin binding. *Science* **323**, 638–41
511 (2009).

512 11. Yao, M. *et al.* The mechanical response of talin. *Nat. Commun.* **7**, 11966 (2016).

513 12. Yang, B. *et al.* Mechanosensing Controlled Directly by Tyrosine Kinases. *Nano Lett.*
514 acs.nanolett.6b02995 (2016) doi:10.1021/acs.nanolett.6b02995.

515 13. Goldmann, W. H. Role of vinculin in cellular mechanotransduction. *Cell Biol. Int.* **40**, 241–256 (2016).

516 14. Bates, E. Ion Channels in Development and Cancer. *Annu. Rev. Cell Dev. Biol.* **31**, 231–247 (2015).

517 15. Gudipaty, S. A. *et al.* Mechanical stretch triggers rapid epithelial cell division through Piezo1. *Nature*
518 **543**, 118–121 (2017).

519 16. Tijore, A. *et al.* Mechanical Stretch Kills Transformed Cancer Cells. *bioRxiv* 491746 (2018)
520 doi:10.1101/491746.

521 17. Bhatt, A., Kaverina, I., Otey, C. & Huttenlocher, A. Regulation of focal complex composition and
522 disassembly by the calcium-dependent protease calpain. *J. Cell Sci.* **115**, 3415–25 (2002).

523 18. Franco, S. J. *et al.* Calpain-mediated proteolysis of talin regulates adhesion dynamics. *Nat. Cell Biol.* **6**,
524 977–83 (2004).

525 19. Franco, S. J. Regulating cell migration: calpains make the cut. *J. Cell Sci.* **118**, 3829–3838 (2005).

526 20. Saxena, M., Changede, R., Hone, J., Wolfenson, H. & Sheetz, M. P. Force-Induced Calpain Cleavage of
527 Talin Is Critical for Growth, Adhesion Development, and Rigidity Sensing. *Nano Lett.* **17**, 7242–7251
528 (2017).

529 21. Travers, T. *et al.* Tandem phosphorylation within an intrinsically disordered region regulates ACTN4
530 function. *Sci. Signal.* **8**, ra51 (2015).

531 22. Yang, B. *et al.* Stopping transformed cancer cell growth by rigidity sensing. *Nat. Mater.* **19**, 239–250
532 (2020).

533 23. Yang, S., Zhang, J. J. & Huang, X. Y. Orai1 and STIM1 Are Critical for Breast Tumor Cell Migration and
534 Metastasis. *Cancer Cell* **15**, 124–134 (2009).

535 24. Clark, K. *et al.* TRPM7, a novel regulator of actomyosin contractility and cell adhesion. *EMBO J.* **25**,

536 290–301 (2006).

537 25. Wei, C. *et al.* Calcium flickers steer cell migration. *Nature* **457**, 901–905 (2009).

538 26. Ellefsen, K. L. *et al.* Myosin-II mediated traction forces evoke localized Piezo1-dependent Ca2+
539 flickers. *Commun. Biol.* **2**, 298 (2019).

540 27. Chen, X. *et al.* A Feedforward Mechanism Mediated by Mechanosensitive Ion Channel PIEZO1 and
541 Tissue Mechanics Promotes Glioma Aggression. *Neuron* **100**, 799-815.e7 (2018).

542 28. McHugh, B. J. *et al.* Integrin activation by Fam38A uses a novel mechanism of R-Ras targeting to the
543 endoplasmic reticulum. *J. Cell Sci.* **123**, 51–61 (2010).

544 29. Coste, B. *et al.* Piezo1 and Piezo2 Are Essential Components of Distinct Mechanically Activated Cation
545 Channels. *Science* **330**, 55–60 (2010).

546 30. Pathak, M. M. *et al.* Stretch-activated ion channel Piezo1 directs lineage choice in human neural stem
547 cells. *Proc. Natl. Acad. Sci.* **111**, 16148–16153 (2014).

548 31. Li, C. *et al.* Piezo1 forms mechanosensitive ion channels in the human MCF-7 breast cancer cell line.
549 *Sci. Rep.* **5**, 1–9 (2015).

550 32. Solis, A. G. *et al.* Mechanosensation of cyclical force by PIEZO1 is essential for innate immunity.
551 *Nature* **573**, 69–74 (2019).

552 33. Borbiro, I., Badheka, D. & Rohacs, T. Activation of TRPV1 channels inhibits mechanosensitive piezo
553 channel activity by depleting membrane phosphoinositides. *Sci. Signal.* **8**, (2015).

554 34. Nourse, J. L. & Pathak, M. M. How cells channel their stress: Interplay between Piezo1 and the
555 cytoskeleton. *Semin. Cell Dev. Biol.* **71**, 3–12 (2017).

556 35. Bavi, N., Richardson, J., Heu, C., Martinac, B. & Poole, K. PIEZO1-Mediated Currents Are Modulated by

557 Substrate Mechanics. *ACS Nano* **13**, 13545–13559 (2019).

558 36. Gaub, B. M. & Müller, D. J. Mechanical Stimulation of Piezo1 Receptors Depends on Extracellular
559 Matrix Proteins and Directionality of Force. *Nano Lett.* **17**, 2064–2072 (2017).

560 37. Albarrán-Juárez, J. *et al.* Piezo1 and G q /G 11 promote endothelial inflammation depending on flow
561 pattern and integrin activation. *J. Exp. Med.* **215**, 2655–2672 (2018).

562 38. Cox, C. D. *et al.* Removal of the mechanoprotective influence of the cytoskeleton reveals PIEZO1 is
563 gated by bilayer tension. *Nat. Commun.* **7**, 1–13 (2016).

564 39. Park, H., Valencia-Gallardo, C., Sharff, A., Tran Van Nhieu, G. & Izard, T. Novel vinculin binding site of
565 the IpaA invasin of Shigella. *J. Biol. Chem.* **286**, 23214–21 (2011).

566 40. Valencia-Gallardo, C. *et al.* Vinculin targeting by Shigella IpaA promotes stable cell adhesion
567 independent of mechanotransduction. *bioRxiv* (2019) doi:10.1101/773283.

568 41. Tullio, A. N. *et al.* Nonmuscle myosin II-B is required for normal development of the mouse heart.
569 *Proc. Natl. Acad. Sci. U. S. A.* **94**, 12407–12412 (1997).

570 42. Elosegui-Artola, A. *et al.* Rigidity sensing and adaptation through regulation of integrin types. *Nat.*
571 *Mater.* **13**, 631–7 (2014).

572 43. Wolfenson, H. *et al.* Tropomyosin controls sarcomere-like contractions for rigidity sensing and
573 suppressing growth on soft matrices. *Nat. Cell Biol.* **18**, 33–42 (2015).

574 44. Robertson, J. *et al.* Defining the phospho-adhesome through the phosphoproteomic analysis of
575 integrin signalling. *Nat. Commun.* **6**, 6265 (2015).

576 45. Byron, A. *et al.* A proteomic approach reveals integrin activation state-dependent control of
577 microtubule cortical targeting. *Nat. Commun.* **6**, 6135 (2015).

578 46. Giannone, G. *et al.* Calcium rises locally trigger focal adhesion disassembly and enhance residency of
579 focal adhesion kinase at focal adhesions. *J. Biol. Chem.* **279**, 28715–28723 (2004).

580 47. Guo, Y. R. & MacKinnon, R. Structure-based membrane dome mechanism for piezo
581 mechanosensitivity. *Elife* **6**, 1–19 (2017).

582 48. Saotome, K. *et al.* Structure of the mechanically activated ion channel Piezo1. *Nature* **554**, 481–486
583 (2018).

584 49. Geng, J. *et al.* A Plug-and-Latch Mechanism for Gating the Mechanosensitive Piezo Channel. *Neuron*
585 **106**, 438-451.e6 (2020).

586 50. Wu, J., Lewis, A. H. & Grandl, J. Touch, Tension, and Transduction – The Function and Regulation of
587 Piezo Ion Channels. *Trends Biochem. Sci.* **42**, 57–71 (2017).

588 51. Murthy, S. E., Dubin, A. E. & Patapoutian, A. Piezos thrive under pressure: Mechanically activated ion
589 channels in health and disease. *Nat. Rev. Mol. Cell Biol.* **18**, 771–783 (2017).

590 52. Lin, Y.-C. *et al.* Force-induced conformational changes in PIEZO1. *Nature* (2019) doi:10.1038/s41586-
591 019-1499-2.

592 53. Tijore, A. *et al.* Biomaterials Selective killing of transformed cells by mechanical stretch. *Biomaterials*
593 **275**, 120866 (2021).

594 54. Dai, J. & Sheetz, M. P. Membrane tether formation from blebbing cells. *Biophys. J.* **77**, 3363–3370
595 (1999).

596 55. Syeda, R. *et al.* Piezo1 Channels Are Inherently Mechanosensitive. *Cell Rep.* **17**, 1739–1746 (2016).

597 56. Giannone, G., Rondé, P., Gaire, M., Haiech, J. & Takeda, K. Calcium oscillations trigger focal adhesion
598 disassembly in human U87 astrocytoma cells. *J. Biol. Chem.* **277**, 26364–26371 (2002).

599 57. Sen, S. & Kumar, S. Combining mechanical and optical approaches to dissect cellular mechanobiology.
600 *J. Biomech.* **43**, 45–54 (2010).

601 58. Cox, C. D., Bavi, N. & Martinac, B. Biophysical Principles of Ion-Channel-Mediated Mechanosensory
602 Transduction. *Cell Rep.* **29**, 1–12 (2019).

603 59. Shi, Z., Graber, Z. T., Baumgart, T., Stone, H. A. & Cohen, A. E. Cell Membranes Resist Flow. *Cell* **175**,
604 1769-1779.e13 (2018).

605 60. Schwartz[1], A., Hall[1], C., Barney[1], L., Babbitt[2], C. & Peyton[1], S. Mechanosensing of Integrin α 6 and
606 EGFR Converges at Calpain 2. (2017) doi:10.1101/164525.

607 61. Sheetz, M. A Tale of Two States: Normal and Transformed, With and Without Rigidity Sensing. *Annu.*
608 *Rev. Cell Dev. Biol.* **35**, annurev-cellbio-100818-125227 (2019).

609 62. Moore, S. W., Roca-Cusachs, P. & Sheetz, M. P. Stretchy proteins on stretchy substrates: the
610 important elements of integrin-mediated rigidity sensing. *Dev. Cell* **19**, 194–206 (2010).

611 63. Galbraith, C. G., Yamada, K. M. & Sheetz, M. P. The relationship between force and focal complex
612 development. *J. Cell Biol.* **159**, 695–705 (2002).

613 64. Roca-Cusachs, P. *et al.* Integrin-dependent force transmission to the extracellular matrix by -actinin
614 triggers adhesion maturation. *Proc. Natl. Acad. Sci.* **110**, E1361–E1370 (2013).

615 65. Ren, X. D., Kiosses, W. B. & Schwartz, M. A. Regulation of the small GTP-binding protein Rho by cell
616 adhesion and the cytoskeleton. *EMBO J.* **18**, 578–585 (1999).

617 66. Gateva, G. *et al.* Tropomyosin Isoforms Specify Functionally Distinct Actin Filament Populations
618 In Vitro. *Curr. Biol.* **27**, 705–713 (2017).

619 67. Valencia-Gallardo, C. *et al.* Cell adhesion promoted by a unique Shigella IpaA vinculin- and talin-
620 binding site. *bioRxiv* 329136 (2018) doi:10.1101/329136.

621 68. Dana, H. *et al.* High-performance calcium sensors for imaging activity in neuronal populations and
622 microcompartments. *Nat. Methods* **16**, 649–657 (2019).

623 69. Donnert, G., Eggeling, C. & Hell, S. W. Major signal increase in fluorescence microscopy through dark-
624 state relaxation. *Nat. Methods* **4**, 81–86 (2007).

625 70. Tinevez, J. Y. *et al.* TrackMate: An open and extensible platform for single-particle tracking. *Methods*
626 **115**, 80–90 (2017).

627 71. McQuin, C. *et al.* CellProfiler 3.0: Next-generation image processing for biology. *PLoS Biol.* **16**,
628 e2005970 (2018).

629 72. Li, J. V. *et al.* Modified N-linked glycosylation status predicts trafficking defective human Piezo1
630 channel mutations. *Commun. Biol.* **4**, 1038 (2021).

631

632 *Figures:*

633 Figure 1

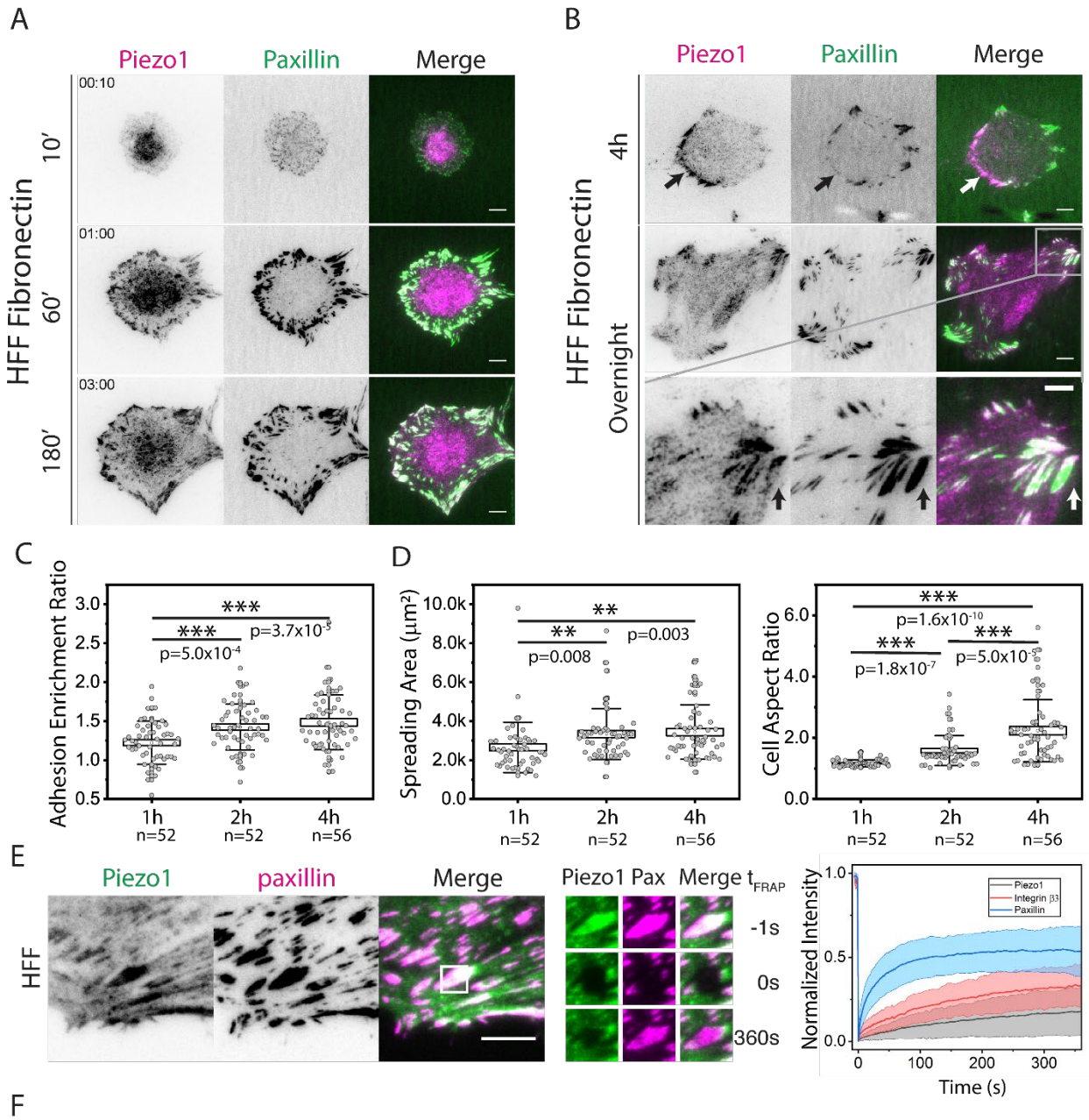

Piezo1 (n=72)		Integrin β3 (n=27)		Paxillin (n=45)	
Mobile Fraction	τ (s)	Mobile Fraction	τ (s)	Mobile Fraction	τ (s)
0.08 [0.07,0.11]	118.0 [104.8,131.2]	0.35 [0.30,0.41]	92.6 [78.5,106.7]	0.60 [0.55,0.63]	25.0 [19.6,30.4]

634

635 **Figure 1. Piezo1 is stably recruited to maturing adhesions on fibronectin surfaces.** (A)Time lapse of cell

636 spreading of HFF cells seeded on fibronectin coated glass surface. The cells are transiently expressing Piezo1-

637 mruby3 and paxillin-BFP. Scale Bars denote 10 um. (B) Localization of Piezo1 spreading on fibronectin
638 surface during polarization and in stable condition. Scale Bars denote 10 um in the main figure and 5um in
639 the zoom. (C) Adhesion enrichment of Piezo1 at 1h, 2h and 4h after cell seeding. The adhesion enrichment
640 was defined as the average intesity ratio of Piezo1 in the adhesions and background. (D) Cell spreading area
641 and aspect ratio 1h, 2h and 4h after cell seeding. The significance were calculated using two sample t-test.
642 (E) Left panel: Live TIRF images of Human Foreskin Fibroblast (HFF) cells transiently transfected with Piezo1-
643 GFP and paxillin-mapple on fibronectin coated surfaces. The adhesion region marked by white square was
644 bleached and snapshots of fluorescent recovery for Piezo1 and talin are shown in the zoom in figure on
645 bottom. Scale Bars denote 5 um. Right panel: The FRAP recovery curve of the bleached region (mean $\pm$ std).
646 (F) The fitted mobile fraction and recovery rates from the FRAP measurements. More than five independent
647 cells and twenty adhesions were picked for each condition. The bracket after the fitting value denote 95%
648 confidence interval of the fitting parameters. In the Frap experiment, Piezo1 is either co-expressed with
649 Integrin β3 or Paxillin.

650 Figure 2

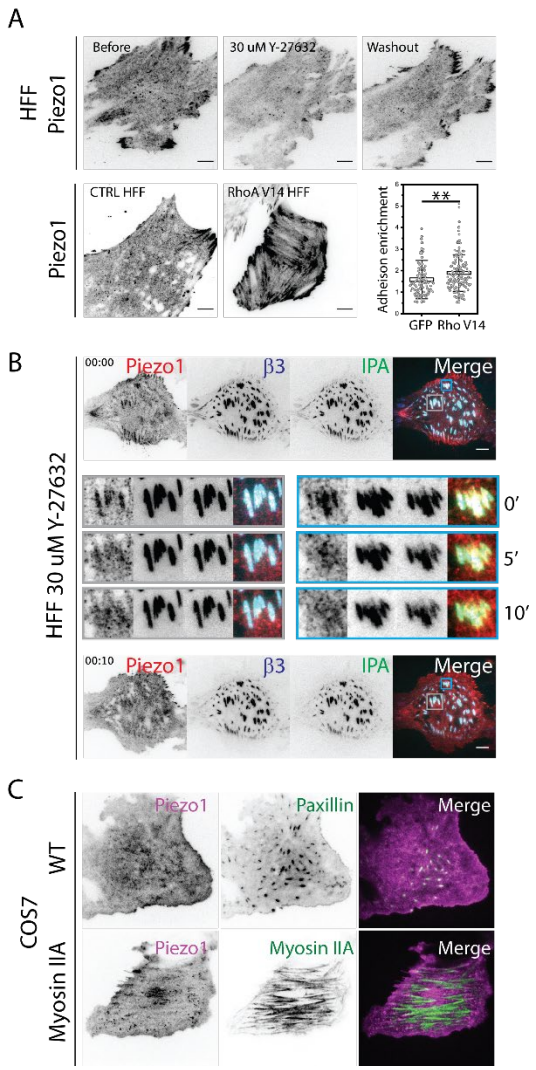

651

652 **Figure 2. Piezo1 localization in HFF cells is controlled by contractility.** (A) Upper panel: Distribution of
653 Piezo1-mRuby3 in HFF cells 15 min after treatment with 30 uM Y-compound and 30 min after washout.
654 Experiments were repeated on > 5 cells with similar results. Lower panel: representative Piezo1 localization
655 and Piezo1 adhesion enrichment quantification in control HFF cells and HFF cells expressing constitutive-
656 active RhoA V14 mutant. Scale Bars denote 10 µm. (B) Time-lapse image of HFF cells transfected with
657 Piezo1-mruby3, integrin β3-Emerald and IPA-GFP with the addition of 30 µM Y-27632. Experiments were
658 repeated on > 3 cells with similar results. (C)Fluorescence image of Piezo1-GFP in COS7 cells with/without
659 overexpressing myosin IIA-mCherry.

660 Figure 3

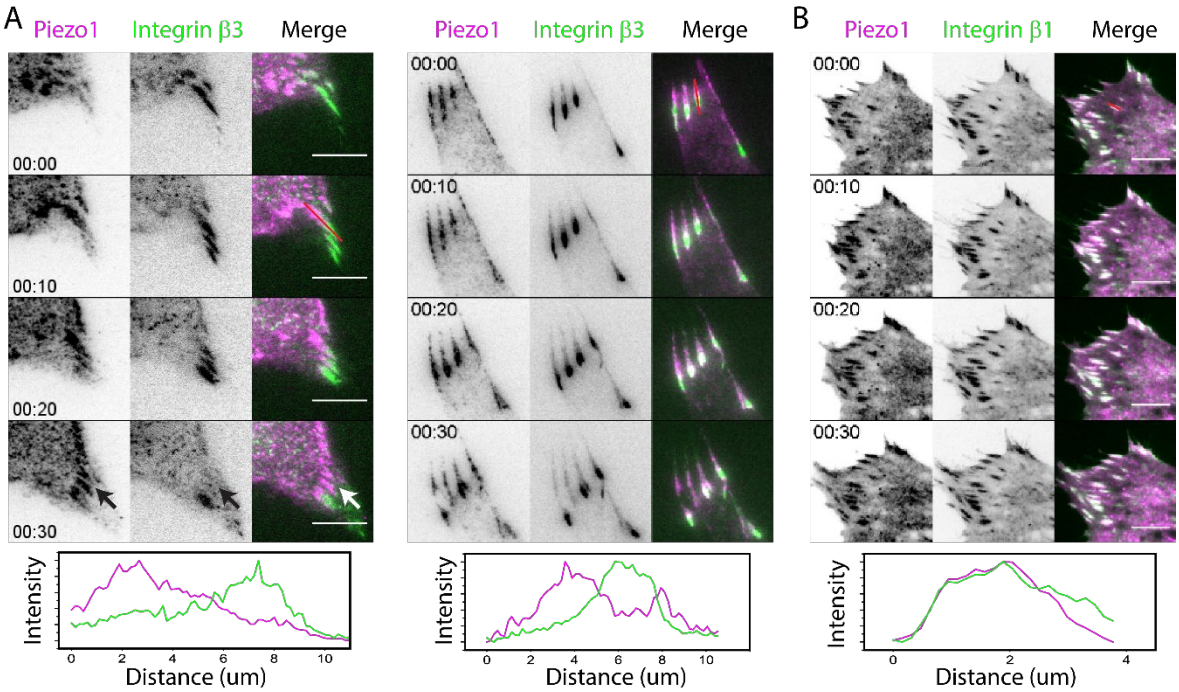

661

662 **Figure 3. Piezo1 recruitment of adhesions precede integrin β3 disassembly.** (A) Kymographs of HFF cells

663 co-transfected with Piezo1-mruby3 and mEmerald-Integrin β3 spreading on fibronectin surfaces. Left panel:

664 A spreading cell one hour after seeding. Right panel: A retracting cell after overnight seeding. (B)

665 Kymographs of HFF cells transfected with Piezo1-mruby3 and mEmerald-Integrin β1 spreading on fibronectin

666 surfaces overnight. The normalized intensity profile of adhesions highlighted by the red line were shown

667 below the figure.

668 Figure 4

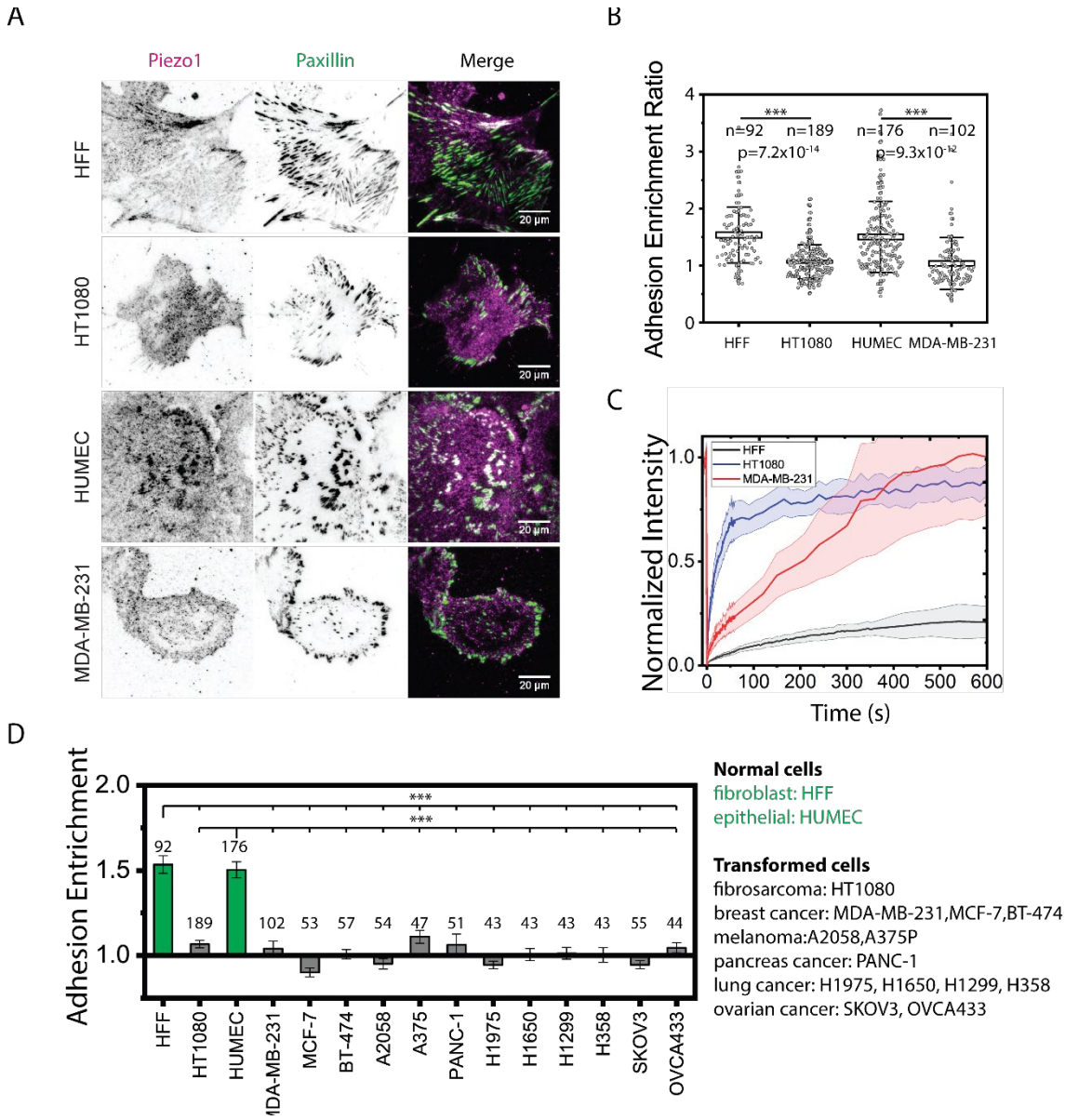

669

670 **Figure 4. Piezo1 localizes to the adhesions of non-transformed cells but is diffusive in transformed**

671 **cells.** (A) Immunostaining of Piezo1 localization in paired normal and transformed cell lines with similar

672 orgin. (B) Quantification of Piezo1 adhesion enrichment for cells in Figure (A). p-values were calculated using

673 two-sample t-test. (C) FRAP recovery curve of Piezo1 in HFF cells and transformed HT1080 and MDA-MB-231

674 cells. The error bar denotes 95% confidence interval of the mean. (D) Quantification of adhesion

675 entrichment of Piezo1 across various normal and transformed cancer cell lines. Error bars denote standard

error of the mean. There were statistically significant differences (p-value < 0.001) between HFF/HUMEC and all the cancer cells.

679

680

681 Figure 5

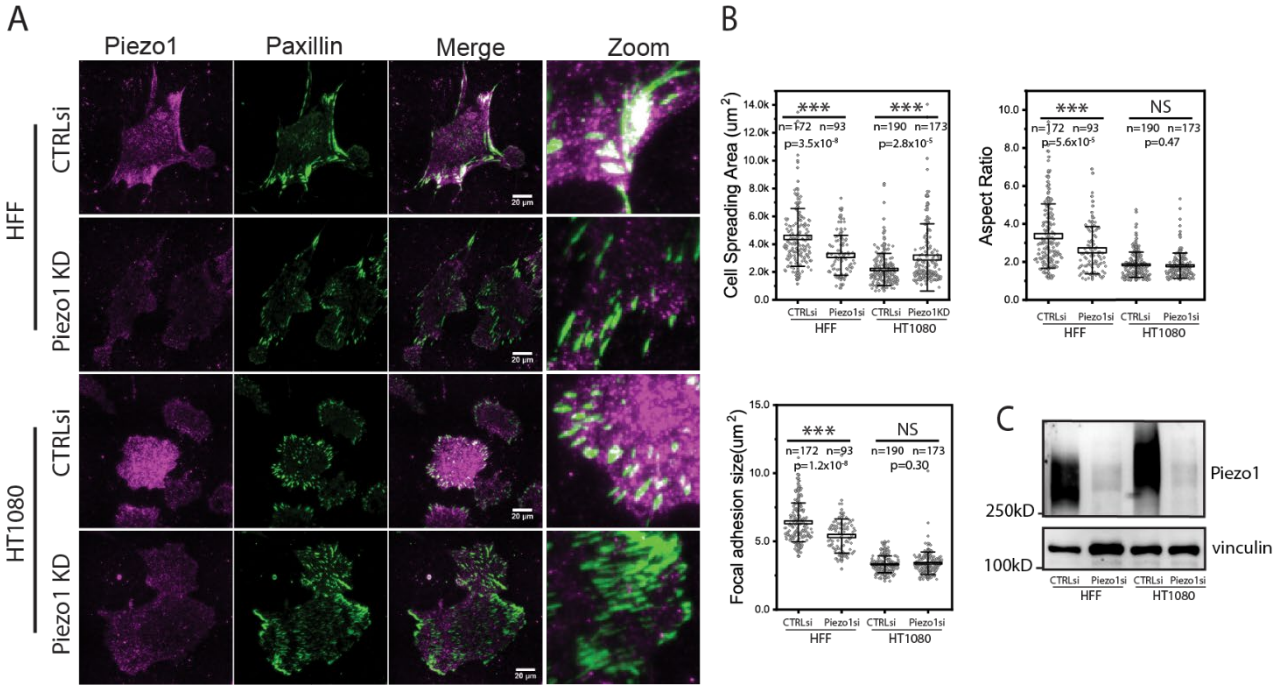

682

683 **Figure 5. Piezo1 localization affects adhesion maturation and correlates with transformation states of**

684 **cells.** (A) TIRF image of fixed cell staining of non-transformed HFF cell line and transformed fibrosarcoma

685 HT1080 with/without Piezo1 knock down after overnight spreading on fibronectin surfaces. Scale Bars

686 denote 20 um. (B) Box plots of the cell spreading areas, cell aspect ratio and mean adhesion sizes of the cells

687 in figure A. Box and error bar denotes the s.e.m and s.t.d of the measurements. The significance value were

688 calculated using two sample t-tests. (C) Western blots of Piezo1 level in control siRNA and piezo1 knock-

689 down cells.

690

691 Figure 6

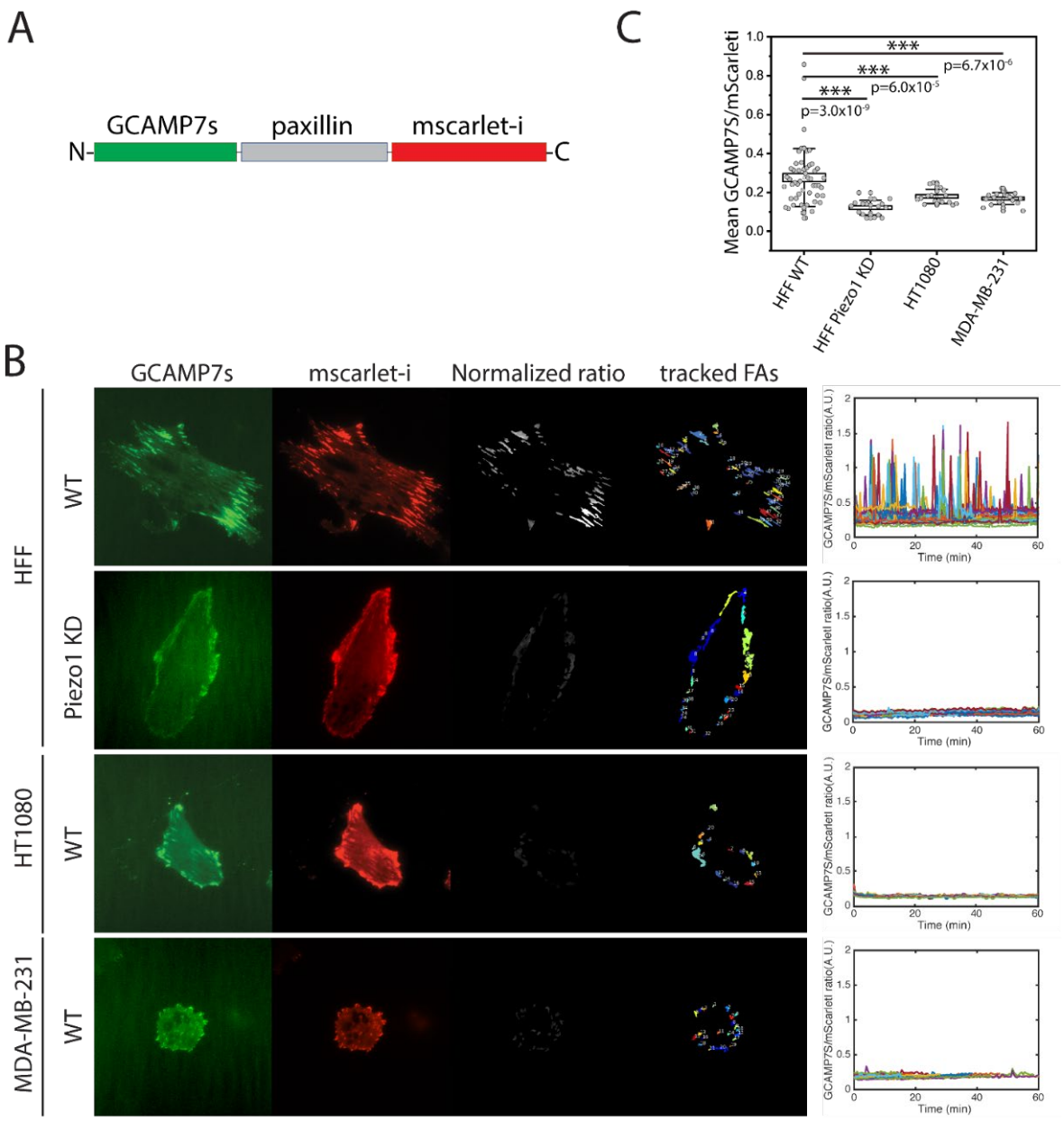

692

693 Figure 6. Normal and transformed cells have distinct adhesion calcium signals . (A) Domain Illustration of

694 the novel adhesion targeting calcium sensor based on jGCaMP7s from Janelia. (B) Left: TIRF image montages

695 of representative HFF cells (with/without Piezo1 knock down), HT1080 and MDA-MB-231 cells transfected

696 with paxillin calcium sensor. The cells were seed on fibronectin surfaces overnight before imaging.

697 Normalized ratio represents the ratio image between jGCaMP7s and mScarlet-I, which is an measure of local

698 Ca^{2+} concentrations. Right: calcium level fluctuations over time in the tracked adhesions of the cell presented

699 in the left panel, each line in the image denotes a single adhesion. The interval of measurement is 30 s. (C)

700 Quantification of average calcium ratio in tracked adhesions over 60 min for different cell types.

701

702 Figure 7

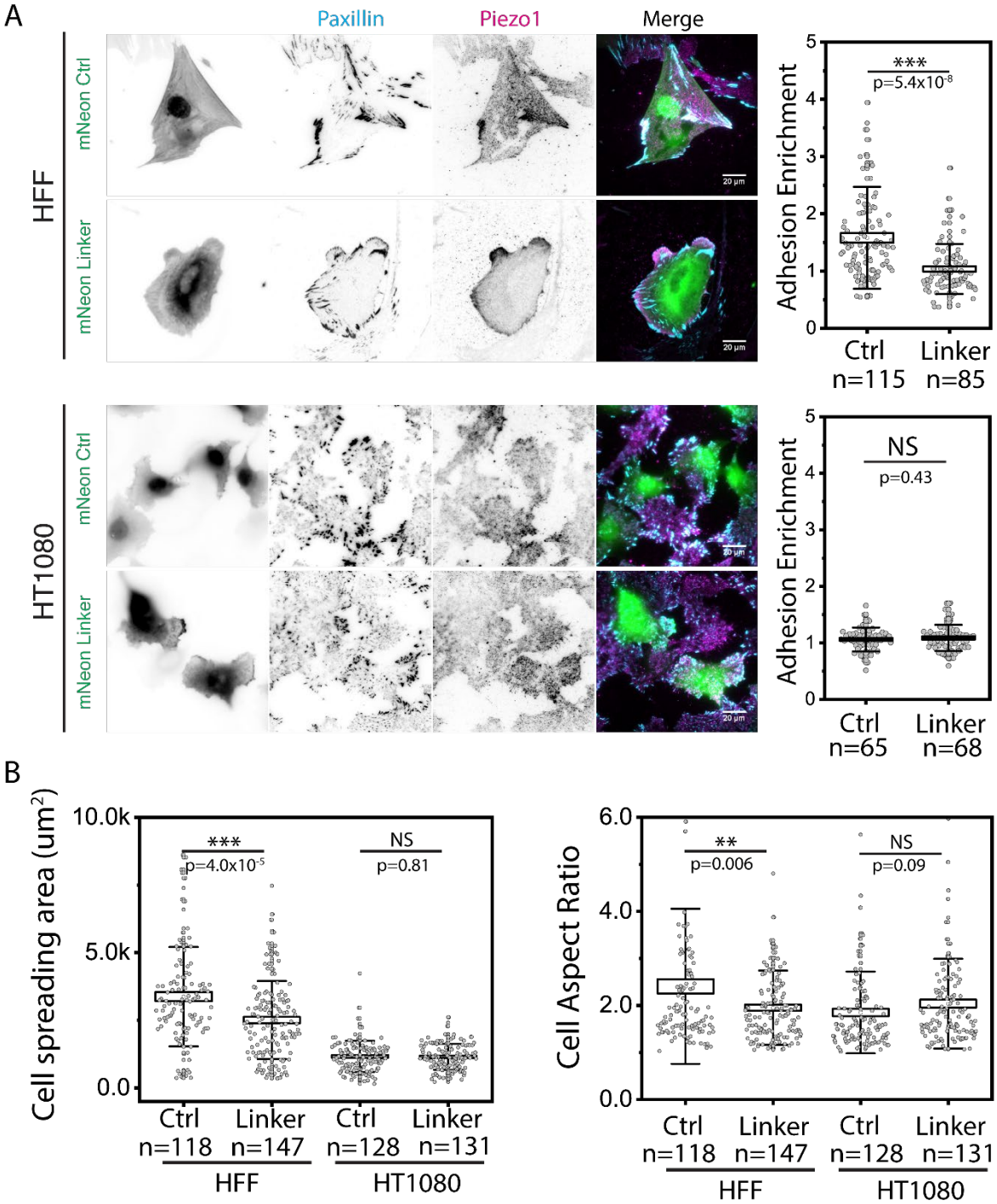

703

704 Figure 7, The linker domain of Piezo1 is linked to adhesion recruitment and alters cell morphology in HFF

705 cells. (A) Immunostaining of HFF and HT1080 cells transfected with mNeongreen control vector or

706 mNeongreen labeled Piezo1 linker construct. The cells were seeded on fibronectin surface overnight and

707 stained with paxillin and Piezo1. (B) Box plot of cell spreading area and cell aspect ratio of positively

708 transfected cells. Box and error bar present s.e.m and s.t.d respectively. Statistical significance were

709 calculated using two sample t-test.

710

711 Figure 8

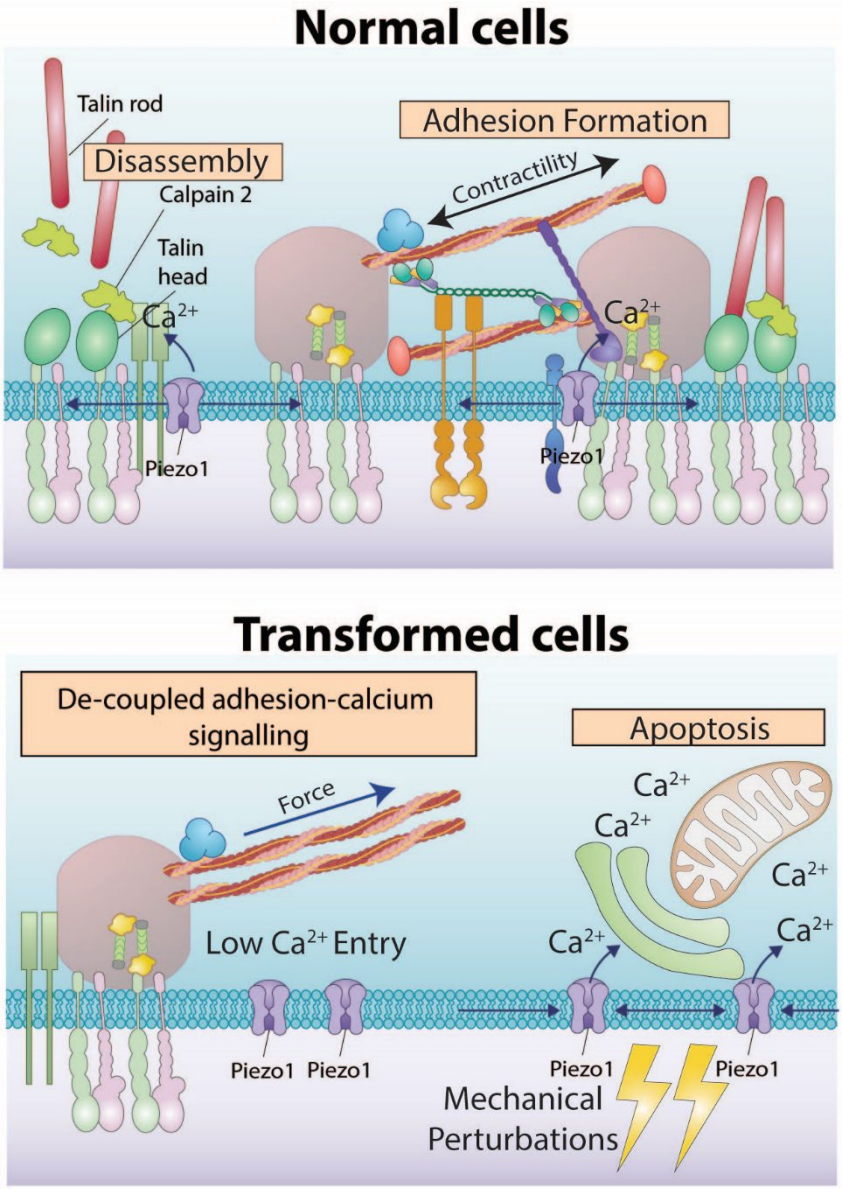

712

713 **Figure 8, Model of the Piezo1's regulation in normal and transformed cells.** (Top Panel) In normal cells,

714 Piezo1 is recruited to maturing focal adhesions in a force dependent manner, where it regulates both the

715 growth and turnover of focal adhesions. (Bottom Panel) In transformed cells Piezo1's localization is diffusive

716 and it no-longer regulate adhesion morphology, which might contribute to the mis-regulated calcium

717 signaling observed in cancer cells including stretch dependent apoptosis[16].

718

719

720 *Supplementary Figures*

721 Figure S1

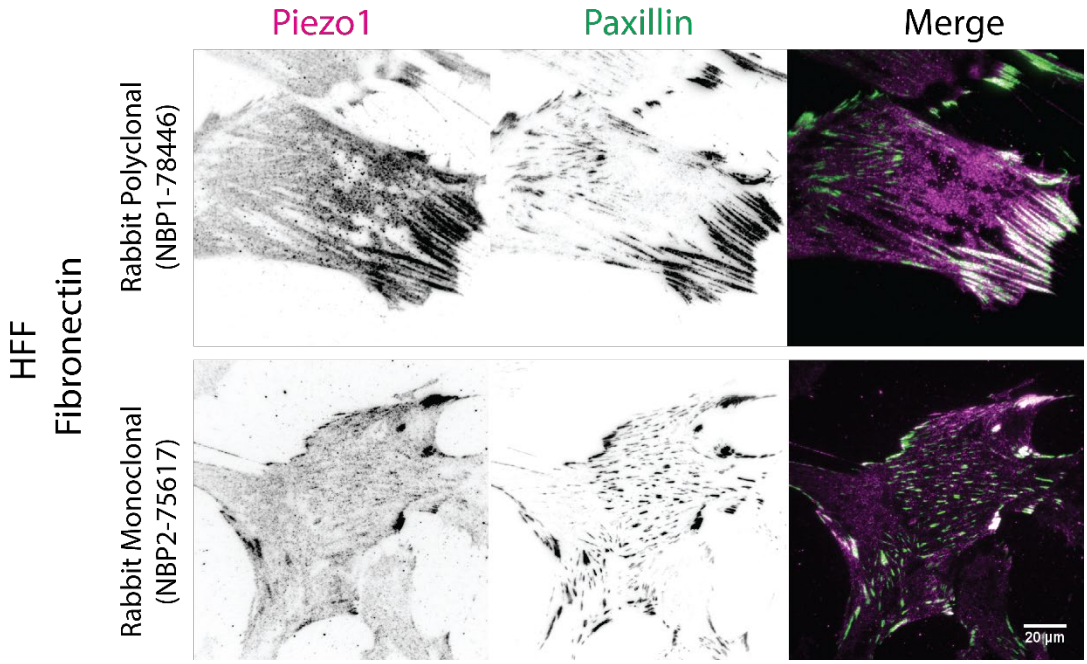

722

723 **Figure S1, Immunostaining of Piezo1 localization of HFF cells.** HFF cells were seeded on fibronectin surfaces

724 overnight, fixed with paraformaldehyde and stained for Piezo1 with two validated Piezo1 antibody and

725 paxillin.

726 Figure S2

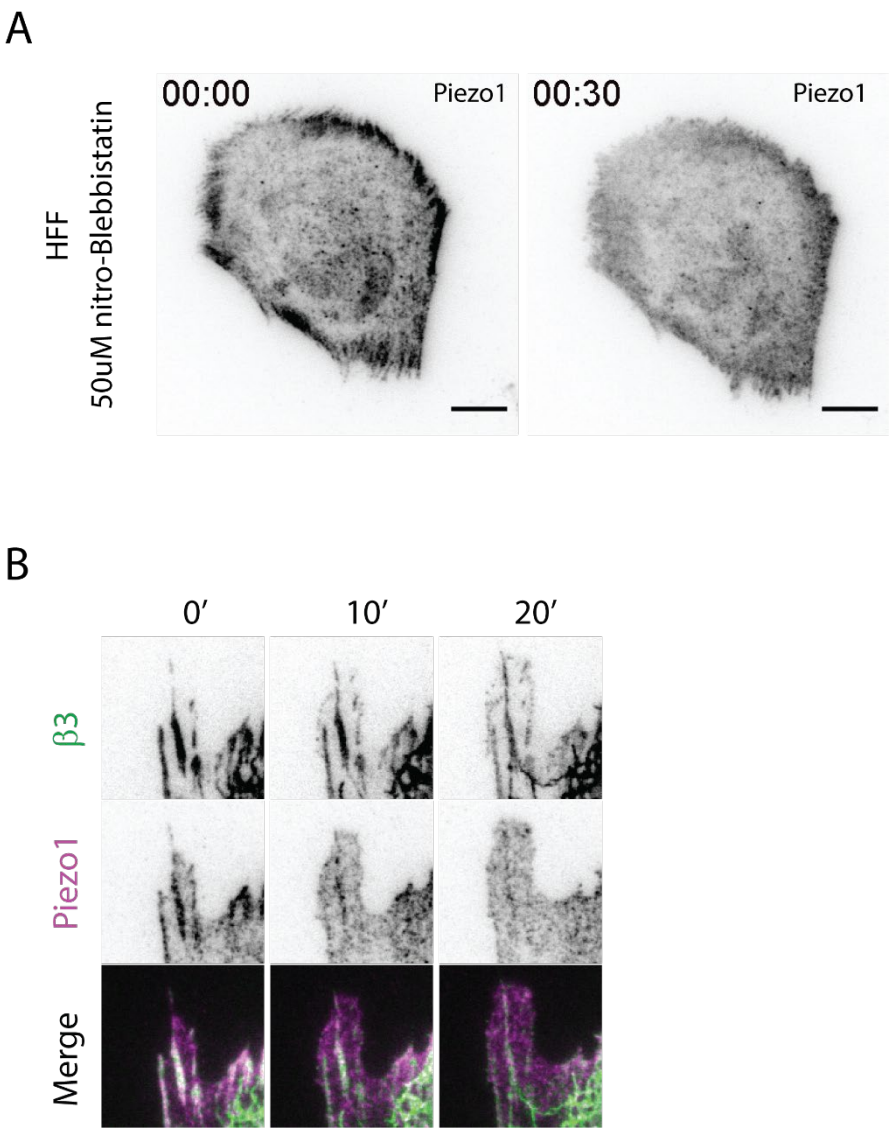

727

728 **Figure S2.** (A) HFF cells transiently transfected with Piezo1-mruby3 were treated with 50 uM nitro-
729 Blebbistatin at time 0. After 30 min incubation, the localization of piezo1 at focal adhesions were lost. Scale
730 Bars denote 10 um. (B) HFF cells transiently transfected with mEmerald-integrin β3 and Piezo1-mruby3
731 were pre-treated with 2.5 uM PTP-PEST inhibitor that inhibits adhesion turnover by phosphatases before
732 addition of 20 uM Y-27632. In this condition, Piezo1 dissociated from adhesions before integrin β3 upon
733 tension release.

734

735 Figure S3

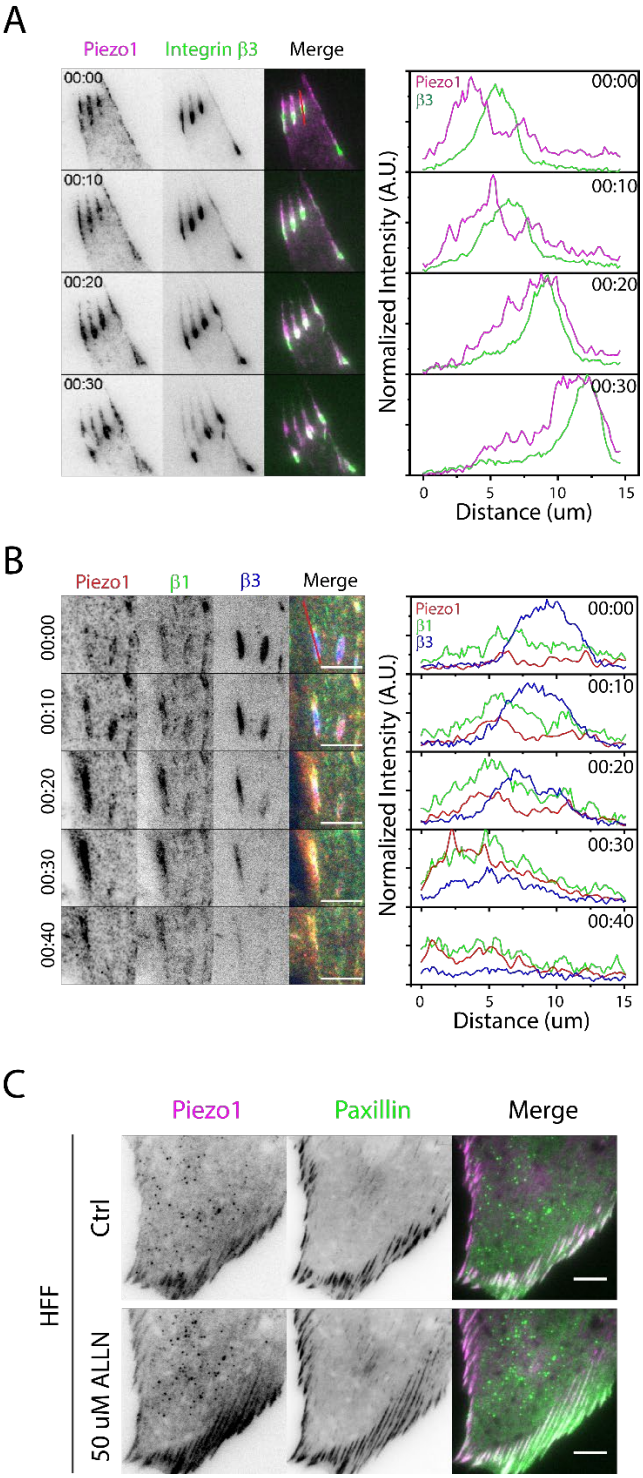

736

737 **Figure S3. Dynamics of Piezo1 localization in relation to integrins.** (A) Adhesion time lapse HFF cells

738 transiently transfected with mEmerald-integrin β3 and Piezo1-mruby3. The right panel showed normalized

739 intensity profiles of the adhesions marked by red line over time. (B) Adhesion time lapse of HFF cells

740 transfected with BFP-integrin β3, mEmerald-integrin β1 and Piezo1-mruby3. The right panel showed
741 normalized intensity profiles of the adhesions marked by red line over time. The normalizations were done
742 by dividing the intensity profiles by the maximum intensity value observed for each protein in the whole
743 time series. Scale Bars denote 10 µm. . (C) Elongation of Piezo1 containing adhesions upon calpain
744 inhibition. Live imaging of HFF cells before and four hours after treatment with 50 µM ALLN. The adhesions
745 were marked by paxillin-mapple. Scale Bars denote 10 um.

746

747 Figure S4

748

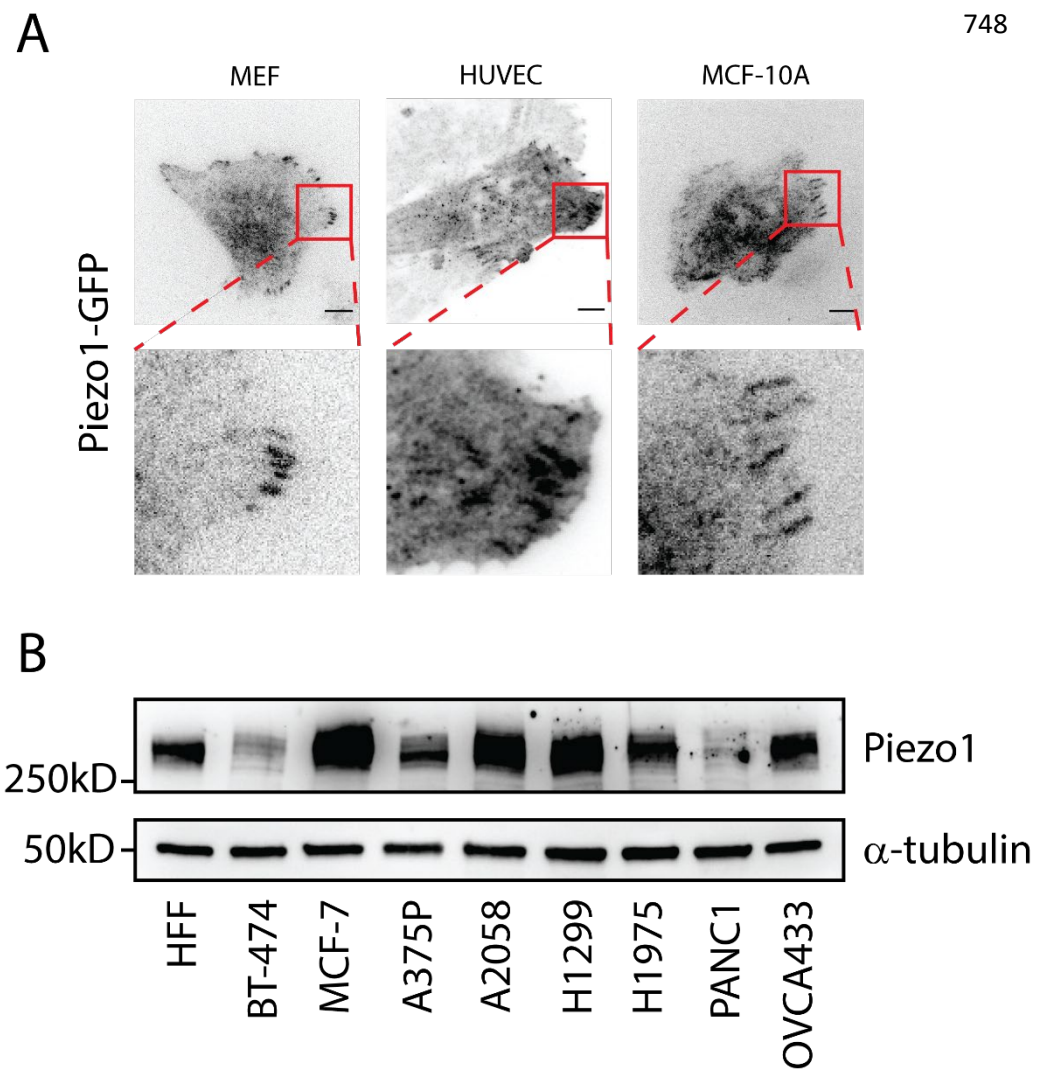

749

750 **Figure S4** (A) TIRF live images of Piezo1-GFP localization in more normal cell lines tested. (B) Western

751 blot images of Piezo1 expression in various cancer cell lines compared against HFF cells.

752

753 Figure S5

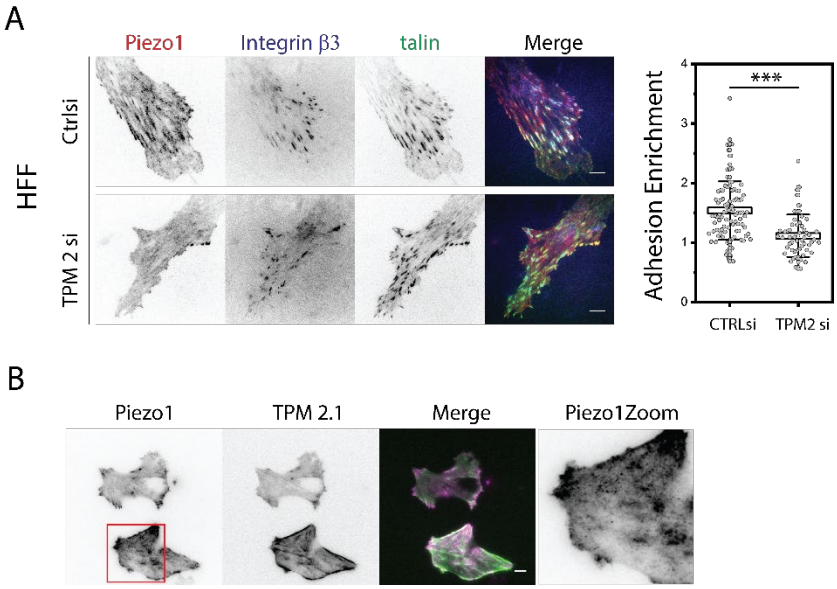

754

755 **Figure S5. Piezo1 localization in cells with altered transformation state.** (A) Representative HFF cells

756 with Control siRNA and TPM 2 siRNA knock down were transfected with Piezo1-mruby3, Integrin β3-BFP and

757 talin-GFP. The cells were seeded on fibronectin surfaces overnight and imaged by TIRFM. Right Panel:

758 quantification of adhesion enrichment with Ctrlsi an d TPM2 si (C) Transient expression of TPM 2.1 -YFP in

759 MDA-MB-231 cells led to the recruitment of Piezo1 to the end of stress fibres decorated by TPM 2.1 (TOP

760 panel). The images present representative cells out of > 20 imaged. Scale Bars denote 10 um.

761

762 Figure S6

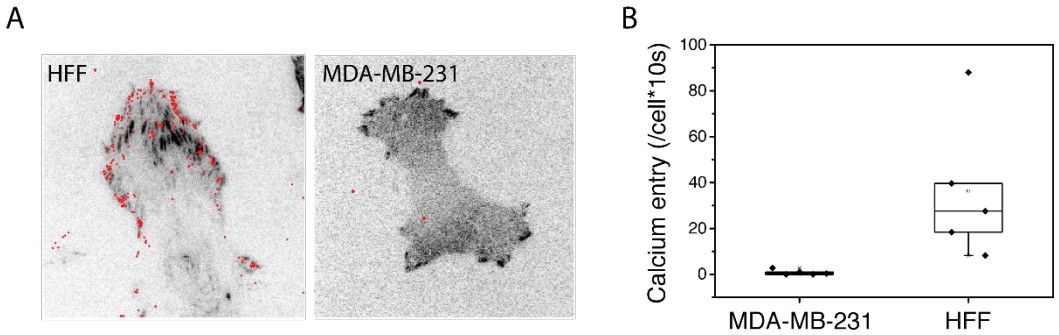

763

764 **Figure S6 HFF and MDA-MB-231 cells showed distinct local calcium entry pattern**. (A) Locations of local
765 calcium entry events (marked by red dots) in HFF cells and MDA-MB-231 cells measured at 100 frames/s for
766 50s, overlaid with focal adhesions marked by paxillin. Significantly more local calcium signal is observed in
767 HFF cells. (B). Box plot of the rate of local calcium events per cell for HFF and MDA-MB-231 cells. Each point
768 denotes an independent cell.

769

770

771

772 Figure S7

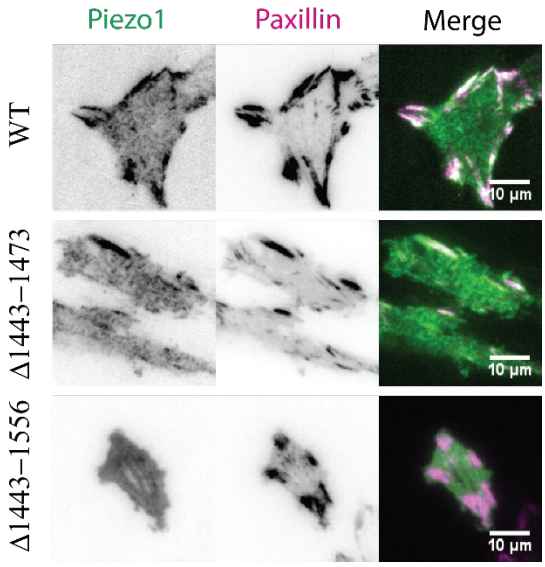

773

774 **Figure S7 Linker domain mutants of Piezo1**. Representative images of FAK-/- MEF cells transfected with

775 paxillin-mapple and wild type/linker deletion mutant of Piezo1. Similar behavior were observed in 3

776 biological repeats with > 10 cells for each condition.

777